Spin-charge separation in the t-J model: Magnetic and transport anomalies

Z.Y. Weng, D.N. Sheng, and C.S. Ting
Texas Center for Superconductivity and Department of Physics, University of Houston, Houston, Texas 77204-5506
(Received 25 January 1995)

A real spin-charge separation scheme is found based on a saddle-point state of the t-J model. In the one-dimensional (1D) case, such a saddle-point reproduces the correct asymptotic correlations at the strong-coupling fixed point of the model. In the two-dimensional (2D) case, the transverse gauge field confining spinon and holon is shown to be gapped at *finite doping* so that a spin-charge deconfinement is obtained for its first time in 2D. The gap in the gauge fluctuation disappears at half-filling limit, where a long-range antiferromagnetic order is recovered at zero temperature and spinons become confined. The most interesting features of spin dynamics and transport are exhibited at finite doping where exotic *residual* couplings between spin and charge degrees of freedom lead to systematic anomalies with regard to a Fermi-liquid system. In spin dynamics, a commensurate antiferromagnetic fluctuation with a small, doping-dependent energy scale is found, which is characterized in momentum space by a Gaussian peak at $(\pi/a, \pi/a)$ with a doping-dependent width ($\propto \sqrt{\delta}$, δ is the doping concentration). This commensurate magnetic fluctuation contributes a non-Korringa behavior for the NMR spin-lattice relaxation rate. There also exist a characteristic temperature scale below which a pseudogap behavior appears in the spin dynamics. Furthermore, an incommensurate magnetic fluctuation is also obtained at a *finite* energy regime. In the transport, a strong short-range phase interference leads to an effective holon Lagrangian which can give rise to a series of interesting phenomena including linear-T resistivity and a T^2 Hall angle. We discuss the striking similarities of these theoretical features with those found in the high-T_c cuprates and give a consistent picture for the latter. Electronic properties like Fermi surface and superconducting pairing in this framework are also discussed.

I. INTRODUCTION

The normal state of high-T_c cuprate superconductors has shown peculiar properties in both charge and spin channels. In the transport aspect, the resistivity[1] exhibits a linear-temperature dependence up to 1000 K and down to a temperature $\simeq T_c$, which can be as low as 10 K. This temperature dependence has been related to a scattering rate[2] that behaves like $\eta \frac{k_B}{\hbar} T$ with $\eta \sim 2$ for all the optimally doped cuprates with T_c ranging from 10 up to over 100 K (a linear-frequency dependence of the scattering rate at frequency $> k_B T/\hbar$ is also found in infrared spectroscopy[2] up to 0.15 eV). Such a linear-T longitudinal resistivity is also accompanied by a Hall coefficient[3] which implies holelike charge carriers and shows a $1/T$ dependence in contrast to the T-independent Fermi-liquid case. A Hall-angle experimental analysis[4,5] has demonstrated that the $1/T$ behavior in the Hall coefficient is due to an additional scattering rate in the transverse channel, which behaves like T^2. Most recently, the magnetoresistance has been found to have a T^{-4} temperature dependence,[6] at variance with Kohler's rule. Furthermore, the thermopower has shown a strong doping dependence,[7] which decreases with the increase of doping and even changes sign in the overdoped regime. All of these transport results are anomalous with regard to the canonical phenomena in a conventional Fermi-liquid (FL) system.

Spin magnetic properties have also exhibited a number of anomalies, which persist into the superconducting phases. Two powerful probes of spin dynamics in the cuprates are nuclear magnetic resonance[8] (NMR) and neutron scattering.[9] In the cuprates, the NMR spin-lattice relaxation rate T_1^{-1}, which probes a very small energy scale ($\sim 10^{-4}$ meV), has shown a strong enhancement[8] at low temperature for planar Cu nuclei, in contrast to the usual Korringa behavior in a Fermi liquid. On the other hand, T_1^{-1} for planar O nuclei[8] is more or less close to the Korringa law. The sharp contrast of the NMR T_1^{-1} between the planar Cu and O nuclei strongly suggests[10–15] that the non-Korringa behavior at Cu sites should be caused by antiferromagnetic (AF) correlations among the Cu spins whose effect could be effectively canceled out at O sites. AF spin fluctuations have been also directly measured by inelastic neutron-scattering experiments[9] at higher energies in $La_{2-x}[Sr, Ba]_xCuO_4$ (LSCO) (Refs. 16–18) and $YBa_2Cu_3O_{7-\delta}$ (YBCO) (Refs. 19–21) materials. However, in contrast with more or less universal behaviors in NMR spin relaxation rates, neutron-scattering data have shown distinctive characteristics among these compounds. For example, commensurate AF fluctuations are observed in insulating LSCO systems[16,17] and underdoped YBCO compounds[19,20] with characteristic energy scales much smaller than the exchange energy $J \simeq 120$ meV. But incommensurate AF correlations have been found[18] in metallic LSCO down to an energy scale as low as 1 meV. Nevertheless, recent analyses have revealed[22,23] that the NMR relaxation rates in LSCO

are inconsistent with an incommensurate AF structure at $\omega \simeq 0$. This is because the effect of incommensurate fluctuations could not be well canceled out at O sites, and a *large* non-Korringa signal would leak to the latter, in contradiction with experiment. In optimally doped YBCO, the *absence* of low-energy AF fluctuations in neutron-scattering experiments[21] is also inconsistent with NMR measurements.[8] Thus a consistent explanation of the NMR data and a reconciliation of NMR and neutron scattering are two essential issues in spin dynamics.

Given these anomalous transport and magnetic properties, one would naturally question if a single type of elementary excitation carrying *both* charge and spin could explain them without leading to any intrinsic contradiction. Since the sharp Fermi edge has been well identified in the cuprates by angle-resolved photoemission measurements,[24,25] such low-lying electronlike excitations, if they exist, should always be located near the Fermi surface, whether it is a Fermi-liquid or a marginal-Fermi-liquid (MFL) (Ref. 26) system. The main difference between FL and MFL systems lies in their energy spaces (the broadening of the quasiparticle in the MFL system is linear in energy[26] as compared to ω^2 in the FL case). But in phase space (momentum space), they are facing essentially the same problems.[27] Low-lying states as labeled by momenta are uniformly distributed in momentum space around Fermi surfaces. The only conceivable structure would come from the topology of Fermi surfaces. The question is whether such a structure of Fermi surface (maybe with nesting and a Van Hove singularity) is capable of explaining so many experimental anomalies. In the transport channel, one of the key problems is how to get hole-type charge carriers, since the elementary excitation is of electron type. Even though a special curvature of Fermi surfaces may explain the hole-like sign indicated by the Hall effect, the total charge carrier number could by no means coincide with the hole number as measured with regard to the half-filled insulating parent compound. Many other problems could arise within such a framework. For example, a monotonic decrease of the thermopower[7] from over 100 μV/K down to 0 and even changing sign, when doping is increased from zero to an overdoped level, is difficult to understand here because the phase space is too limited. Even with the presence of a Van Hove singularity, an overall change as estimated by theory [~ 8 μV/K (Ref. 28)] is too small as compared to the experimental value. Without additional structure, a second scattering rate implied[4,5] in the Hall-angle measurements is even more difficult to comprehend, especially the different ways by which it gets into the transverse and longitudinal channels.

In the spin channel, a number of FL and MFL theories[29,27] have been proposed in terms of the geometry of Fermi surfaces. The topology of Fermi surfaces determines the essential characteristics of spin dynamics through a Lindhard-type response function. These theories provide an explanation of incommensurate AF structure[18] in metallic LSCO, but fail to account for other equally important issues. One is about the NMR relaxation rates whose aforementioned distinctive behaviors at planar Cu and O nuclei are difficult to reconcile.[29,27] The fundamental reason is that a Lindhard response function cannot produce a sharp enough AF peak near $(\pi/a, \pi/a)$. Furthermore, the overall width of the AF peak in these theories is generally not sensitive to doping concentration, and one cannot find NMR anomalies at low temperature to be sufficiently enhanced with the decrease of doping as indicated by the experiments.[8] Most seriously, the itinerant picture fails to provide a small AF energy scale, as the only characteristic scale is the Fermi energy ϵ_F. Although a peak at small energy may be introduced by a Van Hove singularity,[29] it is difficult to relate it to a magnetic energy. The exchange energy scale $\sim J$ as indicated in various magnetic measurements, and an even smaller doping-dependent magnetic energy scale found by inelastic neutron scattering,[16–20] is a strong indication that the local spin description of AF fluctuations may be more appropriate than an itinerant picture. This is further supported by the high-temperature T_1^{-1} measurement in LSCO (Ref. 30) which shows that the doping effect is basically evaporated when $T > 600$ K, where T_1^{-1} at finite doping coincides with that of an insulating antiferromagnet, described by localized spins under the Heisenberg model.[31]

Therefore, the phase-space limitation in an itinerant description, which becomes inevitable in a system where fermionic elementary excitations carry both spin and charge, prevents a consistent explanation of the rich phenomena in the high-T_c cuprates. This implies that an electron in the cuprates may be a composite particle, consisting of more elementary excitations which carry spin and charge quanta (spinon and holon) separately. In this way, spinons and holons may find enough phase spaces of their own to account for the experimental anomalies. A spin-charge separation scenario for the cuprates was proposed by Anderson.[32,33] Under this idea, a strong on-site Coloumb repulsion can lead to a split of the energy band with a large Hubbard gap, and thus real charge carriers (holons) in the conduction band will have an equal number as that of doped holes controlled by experiments. It is a significant first step towards understanding the transport properties. However, in order to reconcile with a sharp Fermi edge found by angle-resolved photoemission, a fermionic spinon with a similar Fermi surface has to be assumed.[32] Thus, at least in the spin channel, basic properties should not be very different from conventional FL or MFL theory, which is a serious setback. Later it was further realized[34–37] that there actually exists a strong coupling among spinons and holons, known as a gauge interaction, and such a gauge force plays a role essentially to confine[38] spinons and honons together, like the quark confinement[39] in quantum chromodynamics. In other words, whether there is a real spin-charge separation in a two-dimensional (2D) strongly correlated model is still unclear.

So we are in a paradox situation. Experimental measurements, on the one hand, point to the possibility of a spin-charge separation. Strong-correlation theories, on the other hand, lead to spin-charge confinement. This awkward situation is actually caused by an oversimplified choice to let spinons to have a large Fermi surface, which

undermines a local description for spins. One may argue that in order to recover a correct electron Fermi surface—an experimental constraint—a large spinon Fermi surface would be necessary. But this is not the case even in one dimension, where a real spin-charge separation exists in the Hubbard model and an electron Fermi surface (points) still satisfies[40] the Luttinger volume theorem. Even though usually people may be used to the thinking[41] that a spinon Fermi surface is the reason for an electron Fermi surface in 1D, the various correlations have never been correctly derived under such a picture. In fact, a FL description of spinons is a too rough approximation in 1D. In the strong-coupling (large-U) regime, a correct spin-charge separation description[42] has been established in a path-integral formalism,[43] where an electron is described as a composite particle of a spinon and a holon, *together* with a nonlocal phase-shift field. It is this phase-shift field that helps to recover the right Fermi-surface position. In this formalism, spinons are described by a local spin representation without a Fermi surface, and both spin and density, as well as various electronic correlation functions, have been correctly obtained.[42] An important lesson learned here is that the electronic Fermi surface is no longer essential in a spin-charge separation scheme, and it can be reproduced from a *phase shift* in a correct spin and charge separation scheme. (We note that in 1D another powerful method is the bosonization method[44–47] in the weak-coupling regime. There the non-Fermi-liquid-like low-lying spin and charge processes can be directly described near the *electronic* Fermi points. But its possible generalization to two dimensions has many difficulties and is still under investigation.)

This leads to a new 2D spin-charge scenario for the cuprates. In this scenario, spinons would be free of "duty" to be responsible for the electron Fermi surface, so that they could get sufficient phase-space freedom to describe anomalous spin dynamics. Electronic Fermi surfaces would be produced by an extra phase-shift field associated with the fermion statistics of electrons, and should not be directly related to holons and spinons. This provides a fundamental reason for the Luttinger theorem to be valid even in strong correlations. It also means that a Fermi-surface topology is no longer crucial in determining spin and charge dynamics. That is, the shape of a Fermi surface due to the detailed band structure, which may vary from one material to others in the cuprates, should not be so relevant to the basic spin and charge anomalies in a spin-charge separation framework. Therefore it may well justify using a simple one-band t-J model[32,48,49] to describe the realistic cuprates if a spin-charge separation is indeed present there. It is noted that several interesting experimental features are already known for the t-J model. For example, the spin degree of freedom is described in a local spin representation, which reduces to the Heisenberg Hamiltonian at half-filling and well describes[50,51] the magnetic behaviors in the insulating cuprates. On the other hand, charge carriers in this system are naturally holes as measured from the half-filled insulating phase, which is also a strong indication of the experimental relevance for the model. A spin-charge separation is already well known for such a model in the 1D case.

It is the purpose of the present paper to establish the above-described spin-charge separation scheme within the t-J framework. Like other approximations, we cannot directly prove that this 2D spin-charge separation state is *the* solution of the t-J model. But such a state will satisfy the following important criteria. The transverse gauge fluctuation will be found suppressed in the long-wavelength and low-energy regime so that spinons and holons are indeed deconfined at finite doping (i.e., spin-charge separation). This is in contrast to singular infrared gauge fluctuation[35–37] in the case of a uniform resonating-valence-bond (RVB) state. At the zero doping limit, the gap of the gauge fluctuation will vanish such that the spinons become confined again to form spin-wave excitations. In this case, a long-range AF order will emerge at zero temperature. Furthermore, the present state can also reproduce the correct results in the 1D case, which is an important check of the theory because only in 1D does one have an exact solution.[52]

In the present paper, the effective Hamiltonian describing the spin-charge separation saddle point will be derived in the following form:

$$H_{\text{eff}} = H_s + H_h, \tag{1.1}$$

where H_s and H_h are the spinon and holon Hamiltonians, respectively, defined by

$$H_s = -J_s \sum_{\langle ij\rangle\sigma} \left(e^{i\sigma A^h_{ij}}\right) b^\dagger_{i\sigma} b_{j\sigma} + \text{H.c.}, \tag{1.2}$$

$$H_h = -t_h \sum_{\langle ij\rangle} \left(e^{i[-\phi^0_{ij}+A^s_{ij}]}\right) h^\dagger_i h_j + \text{H.c.} \tag{1.3}$$

Here $b_{i\sigma}$ and h_i are called spinon and holon annihilation operators, respectively, which are connected to the electron operator in Eq. (1.6) below. H_s and H_h in Eqs. (1.2) and (1.3) would resemble a standard tight-binding Hamiltonian if there are no phase fields A^h_{ij}, ϕ^0_{ij}, and A^s_{ij} ($\langle ij\rangle$ refers to two nearest-neighboring sites on the lattice). Here ϕ^0_{ij} [as defined in Eq. (2.45)] represents a π flux threading through each plaquette. A tight-binding model under ϕ^0_{ij} can be easily diagonalized.[53] The most prominent feature in Eqs. (1.2) and (1.3) is the presence of A^s_{ij} and A^h_{ij}, the so-called topological phases. A^h_{ij} is defined by

$$A^h_{ij} = \frac{1}{2} \sum_{l\neq i,j} \text{Im ln} \left[\frac{z_i - z_l}{z_j - z_l}\right] n^h_l, \tag{1.4}$$

with complex coordinate $z_i = x_i + iy_i$ in 2D, and $n^h_l = h^\dagger_l h_l$ as the holon number operator. A^s_{ij} is given by

$$A^s_{ij} = \frac{1}{2} \sum_{l\neq i,j} \text{Im ln} \left[\frac{z_i - z_l}{z_j - z_l}\right] \left(\sum_\sigma \sigma n^b_{l\sigma}\right), \tag{1.5}$$

with $n^b_{l\sigma} = b^\dagger_{l\sigma} b_{l\sigma}$ as the spinon number operator.

The usual gauge coupling, which otherwise would confine spinons and holons together, will be shown to be suppressed and has been neglected in Eq. (1.1). Thus the residual interaction between spinons and holons are solely mediated through A^s_{ij} and A^h_{ij} in Eqs. (1.2) and (1.3). In the 1D case, the complex coordinate z_i is reduced to a 1D variable, and it is easy to show that A^h_{ij} and A^s_{ij} vanish in Eqs. (1.4) and (1.5). Thus spinons and holons are *decoupled* in 1D, and behave just like free particles on their own tight-binding lattices. In the 2D case, however, A^h_{ij} and A^s_{ij} can no longer be gauged away. A^h_{ij} in Eq. (1.4) describes fictitious π-flux quanta attached to holons which are seen only by *spinons* in H_s. Hence A^h_{ij} will play the role to introduce a doping effect into the spin degree of freedom. On the other hand, A^s_{ij} represents π-flux quanta bound to spinons which can be only seen by *holons*. A^s_{ij} will then play the role of a scattering source in holon transport. So in the spin-charge separation scheme, new types of scatterings are present, and we will show in this paper that it is due to these unconventional forces that magnetic and transport anomalies are produced, consistent with those found in the high-T_c cuprates.

Finally, let us outline how an electron is composed of the elementary excitations, holons and spinons, in this scheme. For both 1D and 2D, the electron annihilation operator $c_{i\sigma}$ will be rewritten as

$$c_{i\sigma} = h^\dagger_i b_{i\sigma} \left[e^{-\frac{i}{2}\sum_{l\neq i}\theta_i(l)\left(\sigma n^h_l - \sum_\alpha \alpha n^b_{l\alpha}+1\right)}(-\sigma)^i \right], \quad (1.6)$$

where $\theta_i(l)$ is defined in Eqs. (2.19) and (2.20). The decomposition (1.6) can be understood as a process by which annihilating an electron is equivalent to creating a holon and annihilating a spinon, and, at the same time, inducing overall nonlocal phase shifts [in the brackets of Eq. (1.6)]. There are several ways to interpret the involvement of phase-shift fields in Eq. (1.6). Since the nonlocal fields appearing in Eq. (1.6) resemble the Jordan-Wigner transformation in both the 1D and 2D cases,[54,55] one may interpret them as statistical transmutations. Here $h^\dagger_i$ is a hard-core bosonic operator, and $b_{i\sigma}$ also satisfies the bosonic commutation relation for the same spin index σ but the anticommutation relation for opposite spins (for details see Sec. II). Thus these nonlocal fields in Eq. (1.6) are to guarantee $c_{i\sigma}$ obeying an electronic commutation relation. A deeper physics behind this is related to the phase-shift idea, whose important role in a strongly correlated system was realized by Anderson.[32,41,47] In 1D it has been explicitly shown[56] that an overall adjustment of the system occurs when a hole is doped into a large-U Hubbard chain, in order to retain the Marshall sign rule[57] in the spin degree of freedom which is decoupled from the charge degree of freedom. This adjustment is found to be just represented by a phase shift shown in Eq. (1.6), and it can lead to the correct Luttinger-liquid behavior of the single-electron Green's function. Furthermore, a phase shift in 1D can also be interpreted as reflecting the fact that each holon carries a spin domain wall (see Ref. 42 and Sec. III). Here one important distinction from Anderson's original phase-shift idea is that a many-body phase shift in 1D will not only give rise to the right non-Fermi-liquid behavior, but also *shift* the Fermi surface to a position satisfying the Luttinger theorem. In other words, there is no need to assume a right Fermi surface at the very beginning. In the present scheme, the form of Eq. (1.6) can ensure a large electron Fermi surface for both 1D and 2D. But we shall discuss these electronic properties in a separate paper for the sake of clarity. In that same paper, we also show that when holons and spinons are both Bose condensed, the phase-shift field in Eq. (1.6) will lead to a long-range *pairing* correlation of electrons (i.e., off-diagonal long-range order), and determine the symmetry of the superconducting order parameter. In the present paper, we mainly focus on the spin-charge separation formalism and explore the corresponding spin dynamics and transport properties.

The remainder of the paper will be organized as follows. In Sec. II, we construct the above-described spin-charge separation scheme[58] based on the t-J model. At the half-filling limit, a long-range AF order can be recovered in 2D, while the well-known spin-spin correlation is also obtained in 1D. At finite doping, the gauge fluctuation is shown to be suppressed so that one has a real spin-charge separation. In Sec. III, the spin dynamics in this scheme is studied at finite doping. In 1D, the correct spin correlation is to be reproduced. In 2D, a number of interesting properties are discovered which provide a consistent picture for the anomalous spin properties in the cuprates. In Sec. IV, the transport properties are investigated. We show that there exists an interesting scattering mechanism within the present framework which leads an effective long-wavelength, low-energy Lagrangian. Such a Lagrangian can give rise to a series of exotic transport properties, in excellent agreement with the experimental measurements. Finally, a conclusive summary will be given in Sec. V.

II. SPIN-CHARGE SEPARATION: FORMALISM

In this section, a mathematical formalism of the spin-charge separation state will be constructed based on the t-J model.

A. Slave-boson formalism and mean-field states

According to Anderson[32] and Zhang and Rice,[48] low-energy physics in the cuprates layers may be properly described by a single-band t-J model. The t-J Hamiltonian reads[49]

$$H_{t\text{-}J} = H_t + H_J, \quad (2.1)$$

with a hopping term

$$H_t = -t \sum_{\langle ij\rangle\sigma} c^\dagger_{i\sigma} c_{j\sigma} + \text{H.c.} \quad (2.2)$$

and a superexchange term

$$H_J = J\sum_{\langle ij\rangle}\left(\mathbf{S}_i\cdot\mathbf{S}_j - \frac{n_i n_j}{4}\right), \tag{2.3}$$

in which $\mathbf{S}_i = \frac{1}{2}\sum_\sigma c^\dagger_{i\sigma}(\hat{\sigma})_{\sigma\sigma'}c_{i\sigma'}$ ($\hat{\sigma}$ is the Pauli matrix) and $n_i = \sum_\sigma c^\dagger_{i\sigma}c_{i\sigma}$. The Hilbert space of the Hamiltonian (2.1) is restricted by the no-double-occupancy constraint

$$\sum_\sigma c^\dagger_{i\sigma}c_{i\sigma} \le 1, \tag{2.4}$$

which imposes a strong correlation on electrons.

By using the slave-boson decomposition of the electron operator[59,60]

$$c_{i\sigma} = h^\dagger_i f_{i\sigma}, \tag{2.5}$$

the no-double-occupancy constraint (2.4) can be replaced by an equality constraint

$$h^\dagger_i h_i + \sum_\sigma f^\dagger_{i\sigma}f_{i\sigma} = 1, \tag{2.6}$$

where $h^\dagger_i$ is a bosonic creation operator and $f_{i\sigma}$ is a fermionic annihilation operator, known as holon and spinon operators, respectively. In this formulation, the hopping and exchange terms of the t-J Hamiltonian become

$$H_t = -t\sum_{\langle ij\rangle\sigma} h^\dagger_j h_i f^\dagger_{i\sigma}f_{j\sigma} + \text{H.c.} \tag{2.7}$$

and

$$H_J = -\frac{J}{2}\sum_{\langle ij\rangle\sigma,\sigma'} f^\dagger_{i\sigma}f_{j\sigma}f^\dagger_{j\sigma'}f_{i\sigma'}. \tag{2.8}$$

In obtaining Eq. (2.8), a term $\propto J\delta^2$ (δ is the doping concentration) has been neglected[36] as usual for simplicity.

The advantage of using the slave-particle formulation for the t-J model is that once the initial state satisfies the constraint (2.6), the no-double-occupancy condition can be always preserved under the Hamiltonians (2.7) and (2.8). Thus the constraint (2.6) in the slave-particle representation will not play a crucial role as the constraint (2.4) does in the original Hamiltonians (2.2) and (2.3). Furthermore, in the slave-boson formulation the natural mean-field decouplings usually have a simpler structure at finite doping than those in the so-called slave-fermion, Schwinger-boson formalism.[51]

Various RVB-type mean-field states have been obtained in the slave-boson formulation.[61] The mean-field decoupling of the Hamiltonians (2.7) and (2.8) may be realized by introducing the mean fields

$$\chi^\sigma_{ij} = \langle f^\dagger_{i\sigma}f_{j\sigma}\rangle, \tag{2.9}$$

$$H_{ij} = \langle h^\dagger_i h_j\rangle. \tag{2.10}$$

By neglecting higher-order fluctuations around χ^σ_{ij} and H_{ij}, the mean-field versions of $H_{t\text{-}J}$ can be obtained in the form of $H^{\rm MF}_{t\text{-}J} = H^{\rm MF}_h + H^{\rm MF}_s$, where

$$H^{\rm MF}_h = -t\sum_{\langle ij\rangle\sigma}\chi^\sigma_{ji}h^\dagger_i h_j + \text{H.c.}, \tag{2.11}$$

$$H^{\rm MF}_s = -\frac{J}{2}\sum_{\langle ij\rangle\sigma\sigma'}\left(\chi^{\sigma'}_{ji} + \frac{t}{J}H_{ji}\right)f^\dagger_{i\sigma}f_{j\sigma} + \text{H.c.} \tag{2.12}$$

The constraint (2.6) should be simultaneously relaxed at this level to a mean-field one $\langle h^\dagger_i h_i\rangle + \sum_\sigma\langle f^\dagger_{i\sigma}f_{i\sigma}\rangle = 1$.

As shown by Eqs. (2.11) and (2.12), both $H^{\rm MF}_h$ and $H^{\rm MF}_s$ have similar hopping forms decided basically by one mean field χ^σ_{ij} (usually $H_{ij}\propto\chi^\sigma_{ij}$ at the saddle point). Since χ^σ_{ij} is responsible for both the hopping and antiferromagnetic superexchange strengths in Eqs. (2.11) and (2.12), an optimization of these two competing charge and spin processes may be relatively easy within this framework.

The simplest mean-field state can be obtained by choosing $\chi^\sigma_{ij} = \chi_0$ and $H_{ij} = H_0$, known as the uniform RVB state.[62] Such a state recently has attracted intensive attention, as one has been able to go beyond the mean-field (or saddle-point) approximation by including the phase fluctuations of χ^σ_{ij} and H_{ij} in terms of the gauge-field description.[35–37] A lesson learned from the gauge-theory approach is that a singular transverse gauge fluctuation could become very important, which implies that spinons and holons are usually confined[38] by a gauge field, as opposed to the artificial decomposition of the electron operator in scheme (2.5). Nonconventional transport phenomena have been discussed[36,37] in this framework which are both theoretically and experimentally interesting.

The uniform RVB state is presumably energetically favorable at a sufficiently large doping. On the other hand, when it is close to half-filling and the doping concentration δ is low, the uniform RVB state may not be an appropriate saddle-point state because the antiferromagnetic energy could be underestimated. For example, at the half-filling limit with $\delta\to 0$, the variational superexchange energy of the uniform RVB state, which can be computed by using the variational Monte Carlo (VMC) method with the no-double-occupancy condition (2.6) being exactly implemented, is found[63] to be $-0.53J$ (per site), about 20% higher than the best ground-state energy $-0.6692J$.[64] Furthermore, no AF long-range order would appear in this limit as it should be present in the true ground state of $H_{t\text{-}J}$.

A substantial improvement of the variational ground-state energy at half-filling can be realized by introducing a phase to χ^σ_{ij} in Eq. (2.9), i.e.,

$$\chi^\sigma_{ij} = \chi_0 e^{i\theta_{ij}}. \tag{2.13}$$

(Note that $H_{ij} = 0$ at $\delta = 0$.) Here the phase θ_{ij} cannot be simply reduced to a difference like $\theta_i - \theta_j$ or, in other words, the summation of θ_{ij} along the closed bonds of a plaquette,

$$\Phi_\square = \sum_\square \theta_{ij}, \tag{2.14}$$

is nonzero. $\Phi_\square$ may be regarded as some fictitious flux

threading through the plaquette. At half-filling, the variational energy is optimized at $\Phi_\square = \pi$, known as the π-flux phase,[53] whose VMC value of the exchange energy is $-0.623J$,[63] only 5% higher than the exact ground-state energy. However, the absence of a long-range AF order in the π-flux phase implies that the long-wavelength, low-energy AF correlations are still underestimated which should predominantly account for the 5% energy missing at this saddle-point state. On the other hand, the high-energy properties of the Heisenberg model, like the temperature dependence of the specific heat, may be well explained in terms of the π-flux phase, as discussed in Ref. 65. (In Ref. 65, the π-flux phase is obtained from a different formulation, involving a 2D Jordan-Wigner transformation[55] of spin-1 operators, instead of the spin-$\frac{1}{2}$ operators used in the present framework.)

Thus, by comparing with the uniform RVB state at half-filling, the short-range AF correlation in the π-flux phase has been substantially improved as a result of the fact that the transverse gauge fluctuation in the former is condensed as the static uniform flux in the latter case. Nevertheless, a lack of long-range AF order in the latter means that the long-range AF correlation is still not appropriately accounted for here. In the following, we will consider a new type of saddle-point state which could retain the high-energy characteristics of the π-flux phase, while properly including the long-wavelength AF correlation in the low-energy regime.

B. Flux binding: New saddle point

In the π-flux phase discussed above, the mean-field Hamiltonian describes a noninteracting fermion gas under some uniform fictitious magnetic field. However, according to exact diagonalizations on a small lattice,[66] such a type of state is generally not energetically favorable as compared to a state in which the uniformly distributed lattice flux is quantized into infinitesimal-size flux tubes, and each of them is bound to an individual particle. The former may be regarded as a "mean-field" version of the latter. In general, the latter is known as an anyon system[67] as the new composites of particles and flux tubes obey different statistics, depending on the flux strength of each flux tube, as compared to the statistics of the underlying particles.

This numerical result is very suggestive here, as in the slave-boson formalism there exists a gauge (phase) degree of freedom which can allow the above flux-binding procedure to happen if it is indeed energetically favorable. This gauge freedom is manifested in the decomposition (2.5), where one may always associate phases $e^{i\theta}$ and $e^{-i\theta}$ to $h_i^\dagger$ and $f_{i\sigma}$, respectively, without changing $c_{i\sigma}$. Such a freedom reflects the arbitrariness of the decomposition (2.5). A gauge field will then play the role of confining any nonphysical spinons and holons together as an electron. Only when one finds a correct spin-charge decomposition, can the gauge fluctuation be expected to get suppressed. Our strategy in the following is to optimize the flux phase by exploiting such a gauge freedom. The main procedure is to regard the uniform fictitious flux as a "mean-field" version of the system where fluxes are quantized and bound to the particles. This latter system may be generally called a flux-binding state. Given the above-discussed uniform π flux, there can be two ways to construct the corresponding flux-binding states at half-filling, as will be outlined below.

Scheme 1. All of $f_{i\sigma}$, no matter their spins, are bound to the same type of flux quanta. When these flux quanta are uniformly smeared out in space, one should recover the uniform flux in π-flux phase. At half-filling, the total number of spinons is one per plaquette on average. Thus each flux tube has to be quantized at π, such that

$$\sum_\square \theta_{ij} = \pi \sum_{l\in\square} \sum_\sigma n_{l\sigma}^f, \tag{2.15}$$

with $n_{l\sigma}^f = f_{l\sigma}^+ f_{l\sigma}$. On average $\langle \sum_\square \theta_{ij} \rangle = \pi$. In this scheme, since each flux tube is quantized at π, spinons are effectively turned into semions[67] (an exchange of two semions gives rise to a phase $\pm i$). Scheme 1 has been already discussed in detail in Ref. 68. Away from half-filling, the mean-field version of this flux-binding state corresponds to the so-called commensurate flux phase (CFP).[69] And the gauge theories[70–73] based on the CFP has a close connection with such a flux-binding state. In both cases, superconducting condensation is found in the ground state, and is related to the semionic condensation.[67] It has been shown in the flux-binding state[68] that there is no explicit time reversal and parity symmetry broken due to the cancellation between charge and spin degrees of freedom. The most interesting features show up in the normal state,[74] which can well explain the anomalous in-plane transport properties in cuprates, including resistivity, the Hall effect, and thermopower. But such a state still has trouble recovering AF ordering at half-filling.

Scheme 2. In this scheme, spinons with opposite spins may not see the flux tubes carried by each other. Thus the flux quantum of each flux tube has to be doubled in order to recover the π-flux phase in the mean-field limit. In this case, the phase θ_{ij} as seen by the spinons with spin index σ has to satisfy the condition

$$\sum_\square \theta_{ij}^\sigma = 2\pi \sum_{l\in\square} n_{l\sigma}^f, \tag{2.16}$$

such that $\langle \sum_\square \theta_{ij}^\sigma \rangle = \pi$ at half-filling. Equation (2.16) means that each spinon is bound to a 2π-flux tube, which would effectively change the spinon statistics from fermion into (hard-core) boson, for spinons with the same spin index σ. In this second flux-binding scheme,[58] the experimental features of the transport properties found in scheme 1 will be essentially retained, while interesting magnetic properties can be also obtained here. As an example, AF long-range order can be recovered at half-filling. Furthermore, the correct 1D behavior is to be reproduced naturally within this framework. All of these suggest that scheme 2 may be a better approximation than scheme 1 for the *same* physical state. Therefore, we shall fully focus on the saddle point of scheme 2 later,

and explore its various properties in the remainder of the paper.

1. Mathematical scheme: Half-filling

At half-filling, H_t has no contribution. One may rewrite H_J in Eq. (2.8) in the form

$$H_J = -\frac{J}{2}\sum_{\langle ij\rangle\sigma\beta}\left(e^{iA^{\sigma}_{ij}}f^{\dagger}_{i\sigma}f_{j\sigma}\right)\left(e^{iA^{\beta}_{ji}}f^{\dagger}_{j\beta}f_{i\beta}\right), \quad (2.17)$$

where a phase A^{σ}_{ij}, which will play a role similar to θ^{σ}_{ij} in Eq. (2.16), is introduced:

$$A^{\sigma}_{ij} = \sigma\sum_{l\neq i,j}[\theta_i(l)-\theta_j(l)]\left(n^f_{l\sigma}-\delta_{\sigma,\uparrow}\right), \quad (2.18)$$

which depends on the positions of spinons nonlocally. This nonlocality is introduced through the multiple-valued phase $\theta_i(l)$:

$$\theta_i(l) = \mathrm{Im}\,\ln(z_i - z_l), \quad (2.19)$$

with $z_i \equiv x_i + iy_i$ in 2D. A vorticity $\pm 2\pi$ can be obtained in $\theta_i(l)$ if the coordinate z_i has been continuously changed around z_l once. In the 1D case, $\theta_i(l)$ in Eq. (2.19) will reduce to

$$\theta_i(l) = \pm\pi\theta(l-i), \quad (2.20)$$

where $\theta(x)$ on the right-hand side is the step function. In obtaining Eq. (2.17), the constraint condition (2.6) has been used, i.e.,

$$\sum_{\sigma} n^f_{i\sigma} = 1, \quad (2.21)$$

at $\delta = 0$.

The identical transformation in Eq. (2.17) has no real physical meaning until the mean-field decoupling scheme is introduced. One may define a hopping operator

$$\hat{\chi}^{\sigma}_{ij} = e^{iA^{\sigma}_{ij}}f^{\dagger}_{i\sigma}f_{j\sigma}. \quad (2.22)$$

Then under the mean field $\chi_0 = \langle\hat{\chi}^{\sigma}_{ij}\rangle$, the saddle-point Hamiltonian of Eq. (2.17) is found as

$$H_s = -J\chi_0\sum_{\langle ij\rangle\sigma} e^{iA^{\sigma}_{ij}}f^{\dagger}_{i\sigma}f_{j\sigma} + \mathrm{H.c.} \quad (2.23)$$

Now the nonlocal field A^{σ}_{ij} appears as a phase in the hopping matrix, which is equivalent to the role of θ_{ij} in Sec. II A.

Two-dimensional case. In terms of Eqs. (2.18) and (2.19), a summation of the phase A^{σ}_{ij} along a plaquette gives

$$\sum_{\square} A^{\sigma}_{ij} = 2\pi\sigma\sum_{l\in\square} n^f_{l\sigma} - 2\pi\delta_{\sigma,\uparrow}. \quad (2.24)$$

Besides a (-2π) lattice flux for $\sigma = \uparrow$, which has no real physical meaning, the right-hand side of Eq. (2.24) implies that each spinon of spin σ carries a flux tube quantized at 2π, with a sign $\sigma = \pm 1$. Since $\langle n^f_{l\sigma}\rangle = 1/2$, one has $\sum_{\square}\langle A^{\sigma}_{ij}\rangle = -\pi$. That is, the "mean-field" version of the saddle-point Hamiltonian (2.23) just corresponds to a π-flux phase Hamiltonian as required (note that $-\pi$ and π fluxes per plaquette are equivalent).

As pointed out before, the flux-binding procedure discussed here is related to a statistics transmutation which is easy to see after introducing a new operator $\bar{b}_{i\sigma}$,

$$\bar{b}_{i\sigma} = f_{i\sigma}e^{-i\sigma\sum_{l\neq i}\theta_i(l)(n^f_{l\sigma}-\delta_{\sigma\uparrow})}. \quad (2.25)$$

Then H_s is reduced to

$$H_s = -J\chi_0\sum_{\langle ij\rangle\sigma}(-\sigma)\bar{b}^{\dagger}_{i\sigma}\bar{b}_{j\sigma} + \mathrm{H.c.} \quad (2.26)$$

One can easily check that $\bar{b}_{i\sigma}$ satisfies the hard-core boson commutation relations (for the same index σ): $[\bar{b}_{i\sigma}, \bar{b}^{\dagger}_{i\sigma}] = 0$ $(i \neq j)$, etc. Of course, for opposite spins one still finds anticommutation relations.

Equation (2.25) resembles the Jordan-Wigner transformation in both the 1D and 2D cases[54,55] which changes the statistics of a fermion into that of a hard-core boson. Thus the presence of a uniform lattice flux in the π-flux phase is a precursor for a fermionic spinon to become a boson. Such a "bosonization" tendency for spinons in the flux phase has been already noted before.[75] The bosonic representation has been known generally to be superior in the description of spin AF correlations.

Equation (2.26) can be further written in the form of a standard hopping Hamiltonian

$$H_s = -J\chi_0\sum_{\langle ij\rangle\sigma} b^{\dagger}_{i\sigma}b_{j\sigma} + \mathrm{H.c.} \quad (2.27)$$

by redefining

$$b_{i\sigma} = (-\sigma)^i\ \bar{b}_{i\sigma}, \quad (2.28)$$

in which $\sigma = \pm 1$ and $(-1)^i = +1$ for the even sublattice and -1 for the odd sublattice of a bipartite lattice. A spin operator like $S^+_i = f^{\dagger}_{i\uparrow}f_{i\downarrow}$ can then be expressed in terms $b_{i\sigma}$ as

$$S^+_i = (-1)^i b^{\dagger}_{i\uparrow}b_{i\downarrow}. \quad (2.29)$$

One also has $S^-_i = (S^+_i)^+$, and $S^z_i = \frac{1}{2}\sum_{\sigma}\sigma b^{\dagger}_{i\sigma}b_{i\sigma}$.

The Bose condensation of $b_{i\sigma}$ at zero temperature as determined by Eq. (2.27) means

$$\langle S^+_i\rangle = (-1)^i\langle b^{\dagger}_{i\uparrow}\rangle\langle b_{i\downarrow}\rangle \neq 0. \quad (2.30)$$

In other words, an antiferromagnetic long-range order in the x-y plane can be indeed obtained in the present flux-binding scheme. The direction of the magnetization in the x-y plane will be determined by the relative phase between the up and down spinons in Eq. (2.30), and could be arbitrary. The evaluation of the magnetization value in Eq. (2.30) needs a detailed knowledge of the hard-core boson behavior governed by H_s. Since we

do not know the exact solution of the hard-core boson Hamiltonian (2.27), we cannot directly estimate the variational ground-state energy of the Heisenberg Hamiltonian H_J in the present saddle-point state. Nevertheless, the ground-state energy for a hard-core boson system like Eq. (2.27) is generally lower as compared to the uniform π-flux system in the fermion representation, which has been discussed by Gros *et al.* in Ref. 76. As pointed out by these authors, the ground-state energy of a hard-core boson system described by H_s could be as much as 11% lower than that in the π-flux phase. Of course, one still needs to check the variational energy of the *original* Hamiltonian H_J in the present saddle-point state. By using a trial bosonic wave function for H_s given in Ref. 76, which is obtained by taking the absolute value of the known fermionic π-flux-phase wave function and gives a 7.4% higher variational energy than the best estimate for H_s, we found analytically that the variational energy of H_J is just identical to that in the π-flux phase. The latter is already known from the VMC calculation, i.e., 5% higher than the exact value of the Heisenberg Hamiltonian. Since the above-mentioned bosonic trial wave function does not have a long-range order (Bose condensation), one may attribute the 5% higher ground-state energy to it. A better bosonic trial wave function of H_s should further improve the variational ground-state energy of H_J.

We note that beyond the present mean-field approximation, a gauge fluctuation should be considered. As will be discussed in Sec. II C, such a gauge fluctuation is not gapped at half-filling and thus could become very important. In fact, spin-1/2 spinons will presumably be confined by the gauge field to form spin-1 excitation (spin wave) at half-filling. This bosonic description is different from the Schwinger-boson representation. The latter has been found[51] to well describe the low-lying spin excitation in 2D half-filling, even at the mean-field level. In contrast, the present scheme will become more powerful in spinon-deconfined cases. For instance, it will be shown later that the gauge fluctuation is to be suppressed at finite doping, and with the presence of spin-charge separation there, the present bosonic representation can become quite convenient to include doping effects. Another spinon deconfinement case is in 1D, which will be discussed below.

One-dimensional case. As a further check of the present saddle-point state, we now turn to the one-dimensional case where the asymptotic spin-spin correlation of the Heisenberg chain has been known for many years.[77]

Under the saddle-point Hamiltonian (2.27), one can write

$$\langle S_i^+(t)S_j^-(0)\rangle = (-1)^{i-j}\langle b_{i\uparrow}^\dagger(t)b_{j\uparrow}(0)\rangle\langle b_{i\downarrow}(t)b_{j\downarrow}^\dagger(0)\rangle. \tag{2.31}$$

In order to evaluate the averages on the right-hand side, the behavior of the hard-core boson described by $b_i(t)$ has to be determined first. A trick which has been often used in 1D is to transform the bosonic operator b_i into a fermionic operator again. By using the expression (2.20) for $\theta_i(l)$ in 1D, $b_{i\sigma}$ is expressed in terms of $f_{i\sigma}$ in Eqs. (2.25) and (2.28) as

$$b_{i\sigma} = f_{i\sigma}e^{\mp i\sigma\pi\sum_{l>i}n_{l\sigma}^f}. \tag{2.32}$$

One also finds that $A_{ij}^\sigma = 0$ in Eq. (2.23), and thus in the fermionic representation H_s simply describes a free lattice fermion gas. Then a correlation function like $\langle b_{i\uparrow}^\dagger(t)b_{j\uparrow}(0)\rangle$ in Eq. (2.31) can be straightforwardly calculated in long time and distance as[78]

$$\langle b_{i\uparrow}^\dagger(t)b_{j\uparrow}(0)\rangle = \langle f_{i\uparrow}^\dagger(t)e^{\pm i\pi\sum_{l>i}n_{l\uparrow}^f(t)}e^{\mp i\pi\sum_{l>j}n_{l\uparrow}^f(0)}f_{j\uparrow}(0)\rangle \propto \frac{1}{[(x_i-x_j)^2-v_f^2t^2]^{1/4}}, \tag{2.33}$$

with $v_f = J\chi_0 a$. The average $\langle b_{i\downarrow}(t)b_{j\downarrow}^\dagger(0)\rangle$ shows the same asymptotic form. Finally by using $(-1)^{i-j} = \cos\frac{\pi}{a}(x_i-x_j)$ and rotational invariance, one obtains

$$\langle \mathbf{S}_i(t)\cdot\mathbf{S}_j(0)\rangle \propto \frac{\cos\frac{\pi}{a}(x_i-x_j)}{[(x_i-x_j)^2-v_f^2t^2]^{1/2}}, \tag{2.34}$$

which describes the correct asymptotic spin-spin correlation in 1D and was first derived by Luther and Peschel from the XXZ model.[77]

Thus the present flux-binding saddle-point state has produced a correct result in 1D, even though it is originally constructed in 2D. This is in contrast to the Schwinger-boson approach,[51] which works rather successfully for the 2D Heisenberg model, but could not predict the correct behavior for the 1D spin-1/2 case. This may be attributed to the fact that spin-1/2 excitations exist in 1D Heisenberg chains, but not in 2D. The present bosonic representation properly describes these spin-1/2 spinons.

We note that in the present approach the spin-spin correlation in the z axis cannot be evaluated at the same level of approximation as in the x-y plane. The reason is that $\langle S_i^z\cdot S_j^z\rangle \sim \frac{1}{4}\sum_\sigma\langle n_{i\sigma}^b n_{j\sigma}^b\rangle$ basically involves the density-density correlation of spinons with the same spin index, while $\langle S_i^+\cdot S_j^-\rangle$ is related to the single-particle propagators of spinons under the saddle point (2.27). The former is generally much harder to evaluate because of the hard-core condition of $b_{i\sigma}$. The 1D correlation $\langle S_i^z\cdot S_j^z\rangle \sim (-1)^{i-j}/|x_i-x_j|$ could be obtained with the hard-core condition being accurately treated through the Jordan-Wigner transformation.

One final point we like to stress here is that H_s in Eq. (2.23) is formally the same as that in the uniform RVB saddle point, since $A_{ij}^\sigma = 0$ in 1D. In other words, flux binding, or statistics transmutation, has no effect on the Hamiltonian in 1D as is well known. What is different between these two saddle-point states is the boundary condition for the fermion $f_{i\sigma}$: In the present saddle point, $f_{i\sigma}$ appearing in Eq. (2.32) will become multiple valued at the boundary once the 1D chain is closed as a loop. As discussed by Shastry,[79] such a boundary condition decides why a hard-core boson system is energetically more favorable than a fermionic gas.

2. *Flux binding: Finite doping*

For a small doping concentration, one expects the antiferromagnetic correlation still to remain dominant, even though it may be strongly modified by doped holes. It is very interesting to see the evolution of the flux-binding saddle-point state in this finite doping case.

We may follow the procedure shown in Sec. II B 1, starting with the identical transformation of H_J in Eq. (2.17). At finite doping, the form of A^{σ}_{ij} in Eq. (2.18) will be slightly modified because the constraint equation (2.21) now is replaced by the full equation (2.6). It is easy to show that A^{σ}_{ij} is given as follows:

$$A^{\sigma}_{ij} = \sigma \sum_{l \neq i,j} [\theta_i(l) - \theta_j(l)] \left(n^f_{l\sigma} - \delta_{\sigma,\uparrow} + \frac{1}{2} n^h_l \right), \quad (2.35)$$

which keeps the identical transformation in Eq. (2.17) unchanged. In Eq. (2.35), an additional factor $n^h_l/2$ is introduced, with $n^h_l = h^{\dagger}_l h_l$ as the holon number operator.

At finite doping, the hopping term H_t in the $H_{t\text{-}J}$ will also contribute, and it may be rewritten in the form

$$H_t = -t \sum_{\langle ij \rangle \sigma} e^{iA^f_{ij}} h^{\dagger}_i h_j \hat{\chi}^{\sigma}_{ji}, \quad (2.36)$$

where $\hat{\chi}^{\sigma}_{ji}$ is defined by Eq. (2.22) with A^{σ}_{ji} given in Eq. (2.35). A^f_{ij} in Eq. (2.36) is a rearranged form of A^{σ}_{ij} after using the constraint (2.6):

$$A^f_{ij} = \frac{1}{2} \sum_{l \neq i,j} [\theta_i(l) - \theta_j(l)] \left(\sum_{\sigma} \sigma n^f_{l\sigma} - 1 \right). \quad (2.37)$$

Note that A^f_{ij} in Eq. (2.37) has no explicit σ dependence.

Now we may take the mean-field decoupling of H_J in Eq. (2.17) and H_t in Eq. (2.36), by introducing the mean fields $\chi_0 = \langle \hat{\chi}^{\sigma}_{ij} \rangle$ and $H_0 = \langle \hat{H}_{ij} \rangle$ (here $\hat{H}_{ij} \equiv e^{iA^f_{ij}} h^{\dagger}_i h_j$). At the same time, the constraint (2.6) has to be relaxed up to a global level, as outlined before. Then the saddle-point Hamiltonian at finite doping is found to be

$$H^{\mathrm{MF}}_{t\text{-}J} = H_s + H_h, \quad (2.38)$$

in which the spinon degree of freedom has the same form as in the half-filling case:

$$H_s = -J_s \sum_{\langle ij \rangle, \sigma} e^{iA^{\sigma}_{ij}} f^{\dagger}_{i\sigma} f_{j\sigma} + \mathrm{H.c.}, \quad (2.39)$$

with $J_s = J\chi_0 + tH_0$. The holon degree of freedom is described by

$$H_h = -t_h \sum_{\langle ij \rangle} e^{iA^f_{ij}} h^{\dagger}_i h_j + \mathrm{H.c.}, \quad (2.40)$$

with $t_h = 2t\chi_0$. t_h and J_s have to be determined self-consistently. Since the averages χ_0 and H_0 actually do not depend on t_h and J_s, the self-consistency should be always satisfied here, even though an actual determination of the values for t_h and J_s is nontrivial. Generally one can estimate $t_h \sim t$ and $J_s \sim J$ at small doping. In the bosonic representation of Eqs. (2.25) and (2.28), H_s can be further expressed as

$$H_s = -J_s \sum_{\langle ij \rangle \sigma} e^{i\sigma A^h_{ij}} b^{\dagger}_{i\sigma} b_{j\sigma} + \mathrm{H.c.}, \quad (2.41)$$

where the topological phase A^h_{ij} is defined by

$$A^h_{ij} = \frac{1}{2} \sum_{l \neq i,j} [\theta_i(l) - \theta_j(l)] \, n^h_l. \quad (2.42)$$

In one dimension, one will find $A^h_{ij} = A^f_{ij} = 0$ in Eqs. (2.40) and (2.41) according to Eq. (2.20). The holon (described by h_i) and spinon (described by $b_{i\sigma}$) degrees of freedom are thus decoupled at this saddle-point state. In two dimensions, however, the holon and spinon are coupled with each other through the nonlocal fields A^f_{ij} and A^h_{ij} in H_h and H_s. The topological gauge field A^h_{ij} can be interpreted as describing fictitious π-flux quanta attached to holons, but only seen by spinons. This becomes clear if one considers an arbitrary loop C, and counts the flux enclosed, which is given by

$$\sum_C A^h_{ij} = \pi \sum_{l \in C} n^h_l. \quad (2.43)$$

A^f_{ij} in Eq. (2.37) may be rewritten as $A^f_{ij} = A^s_{ij} - \phi^0_{ij}$, where

$$A^s_{ij} = \frac{1}{2} \sum_{l \neq i,j} [\theta_i(l) - \theta_j(l)] \left(\sum_{\sigma} \sigma n^b_{l\sigma} \right), \quad (2.44)$$

and ϕ^0_{ij} is defined by

$$\phi^0_{ij} = \frac{1}{2} \sum_{l \neq i,j} [\theta_i(l) - \theta_j(l)], \quad (2.45)$$

which describes a lattice π flux with $\sum_{\square} \phi^0_{ij} = \pi$. The topological gauge field A^s_{ij} describes fictitious π-flux tubes carried by spinons which are seen by holons. In Secs. III and IV, we will investigate how the couplings induced by the nonlocal fields A^h_{ij} and A^s_{ij} will lead to highly nontrivial spin and charge properties in the 2D case.

To end this section, we would like to give a different perspective about the construction of the flux-binding state. Recall that one has a gauge degree of freedom in the slave-boson decomposition: $c_{i\sigma} = h^{\dagger}_i b_{i\sigma} = (h^{\dagger}_i e^{i\theta_h})(f_{i\sigma} e^{i\theta_f})$, where θ_h and θ_f can be *any* phase satisfying $\theta_h + \theta_f = 0$. Particularly, if θ_h and θ_f are chosen as the topological phases in the Jordan-Wigner transformation, statistics transmutation can happen so that one may end up with a slave-fermion or, more generally, slave-anyon decomposition.[68] This is not surprising because all of these formalisms are mathematically equivalent. A very complicated decomposition can be also constructed. Distinctive physics is involved here only when one makes

the mean-field decoupling. In this way, different decompositions mean different saddle-point states. The usual slave-boson and slave-fermion formalisms are the simplest ones, but not necessarily the appropriate ones for the correct saddle point. The present saddle-point state corresponds to $\theta_h = 1/2\sum_{l\neq i}\theta_i(l)[\sigma(1-n_l^h)+\sum_\alpha \alpha n_{l\alpha}^f]$ and $\theta_f = -i\sigma\sum_{l\neq i}\theta_i(l)n_{l\sigma}^f$. It is easy to check that $\theta_h+\theta_f=0$ in terms of the constraint (2.6). Correspondingly, $c_{i\sigma}$ may be rewritten as in Eq. (1.6) where $b_{i\sigma}$ is defined by Eqs. (2.25) and (2.28). In this new decomposition, an electron is composed of two *bosonic* holons and spinons, together with some nonlocal fields. A spin operator like $S_i^+ = f_{i\uparrow}^\dagger f_{i\downarrow}$ can also be expressed as

$$S_i^+ = (-1)^i b_{i\uparrow}^\dagger b_{i\downarrow} e^{i\sum_{l\neq i}\theta_i(l)n_l^h}. \tag{2.46}$$

Its physical meaning will be explored in Sec. III. In the following, we will go beyond the mean-field approximation and show that a real spin-charge separation can be indeed realized with the decomposition (1.6).

C. Gauge-theory description: Spin-charge separation

It is now a well-recognized fact[36,37] that any saddle-point-state properties of the t-J model could be substantially modified by the low-lying gauge fluctuation around the saddle point. So it is very important to check the gauge fluctuations around the present saddle point. Here gauge fluctuations are to be related to phase fluctuations of the mean fields $\langle\hat{\chi}_{ij}\rangle$ and $\langle\hat{H}_{ij}\rangle$. The main idea behind the construction of flux-binding saddle-point states is to incorporate the most singular transverse gauge fluctuations into the saddle point via flux binding so that additional phase fluctuations become insignificant. These singular gauge fields are represented by the topological gauge fields A_{ij}^h and A_{ij}^s in the saddle-point Hamiltonians H_s and H_h. In the following, we will show that the transverse gauge fluctuation around this saddle point is indeed suppressed at finite doping, and therefore we have a real spin-charge separation whose low-energy physics will be determined in terms of the effective Hamiltonians H_s and H_h, defined by Eqs. (1.1)–(1.5) in the Introduction.

An effective Lagrangian, with the constraint (2.6) enforced and the (phase) gauge fluctuation around the present flux-binding saddle-point state included, can be written as[36,68]

$$\mathcal{L}_{\rm eff} = \sum_i\left(\sum_\sigma b_{i\sigma}^\dagger(\partial_\tau-\mu)b_{i\sigma} + h_i^\dagger(\partial_\tau-\mu)h_i\right) + \tilde{H}_{\rm eff}, \tag{2.47}$$

where

$$\tilde{H}_{\rm eff} = -J_s\sum_{\langle ij\rangle\sigma} e^{i(a_{ij}+\sigma A_{ij}^h)}b_{i\sigma}^\dagger b_{j\sigma} + \text{c.c.} \\ -t_h\sum_{\langle ij\rangle} e^{i(a_{ij}+A_{ij}^s-\phi_{ij}^0)}h_i^\dagger h_j + \text{c.c.} \tag{2.48}$$

Here a_{ij} in Eq. (2.48) describe an internal gauge field. Originally the no-double-occupancy constraint (2.6) [with $f_{i\sigma}$ changed to $b_{i\sigma}$ by the transformations (2.25) and (2.28)] is implemented through a Lagrangian multiplier field, whose fluctuating part is then absorbed by the longitudinal part of a_{ij} in Eq. (2.48) due to gauge invariance,[68] with μ left in Eq. (2.47) enforcing the constraint at a global level.

The existence of a gauge freedom in $\mathcal{L}_{\rm eff}$ will guarantee the following current constraint between spinons and holons:[36,68]

$$\mathbf{J}_s = -\mathbf{J}_h. \tag{2.49}$$

It is noted that Eq. (2.49) in a longitudinal channel is a simple reflection of the density constraint (2.6), but its transverse channel has nothing directly to do with the no-double-occupancy constraint, and is related to the property of the t-J Hamiltonian. It is the transverse gauge fluctuation that becomes singular in the long-wavelength, low-energy regime in the uniform RVB state.[36,37] This transverse field would serve as a confining force in a usual non-spin-charge-separation state. The current constraint (2.49) is also connected to the Ioffe-Larkin combination rule[35] of the response to an external electromagnetic field,

$$K_e = [K_s^{-1}+K_h^{-1}]^{-1}, \tag{2.50}$$

where K_s and K_h are the response matrices of spinon and holon systems under effective Hamiltonians H_s and H_h in Eqs. (1.2) and (1.3).

In gauge theory, the dynamics of the gauge field a_{ij} is determined after the spinon and holon degrees of freedom are integrated out.[35,36] When the gauge fluctuation is weak, one may use the Gaussian approximation, and the gauge-field propagator $D_{\mu\nu}^a = -\langle T_\tau a_\mu a_\nu\rangle$ ($\mu,\nu = x, y$) in imaginary time can be determined by[35,36]

$$D^a = -[K_s+K_h]^{-1} \tag{2.51}$$

in imaginary-frequency space. In the present system, holons are under some fluctuating flux described by A_{ij}^s (cf. Sec. IV), and its response function will follow the usual metallic $\mathbf{q}$ and ω dependences:[35] $i\omega\sigma_h - \chi_h q^2$. The most interesting behavior will come from the spinon part K_s as discussed below.

In the spinon part of $\tilde{H}_{\rm eff}$, there is a sign $\sigma = \pm 1$ in front of the topological phase A_{ij}^h. This sign means that spinons with $\uparrow$ and $\downarrow$ spins see the fictitious flux quanta carried by holons in opposite directions. Since there is no such sign in front of the gauge field a_{ij}, a nonzero a_{ij} will then polarize the spinon system with regard to spin σ. This polarization is generally energetically unfavorable, and we expect a suppression of the gauge field a_{ij} to stabilize the system.

A mathematical demonstration is straightforward. As will be discussed in Sec. III, one may rewrite A_{ij}^h as $A_{ij}^h = \bar{A}_{ij}^h + \delta A_{ij}^h$, where $\bar{A}_{ij}^h$ is a "mean field" with the flux quanta uniformly smeared out in space. A uniform fictitious magnetic field $B_h = \pi\delta/a^2$ will correspond to such a vector potential $\bar{A}_{ij}^h$. On the other hand, δA_{ij}^h will be correlated with the holon density fluctuation. If one

integrates out the spinon degree of freedom (under the "mean field" $\bar{A}^h_{ij}$) in $\mathcal{L}_{\rm eff}$, an effective action for quadratic fluctuation of the gauge field is found by

$$S_s[a,\delta A^h] = \frac{1}{2}\sum_\sigma \left(a+\sigma\delta A^h\right)\Pi_\sigma\left(a+\sigma\delta A^h\right), \quad (2.52)$$

where Π_σ is the response matrix of spinon σ under a fictitious magnetic field σB^h. K_s will be determined through $S_s = \frac{1}{2}aK_sa$,[70] and one needs to further integrate out δA^h in Eq. (2.52). As a first step, if one neglects the δA^h dynamics, by directly integrating out δA^h in Eq. (2.52), the following expression for K_s can be obtained:

$$K_s = 4\left[\Pi_\uparrow^{-1}+\Pi_\downarrow^{-1}\right]^{-1}. \quad (2.53)$$

The key thing here is that the up and down spinons see the opposite fictitious magnetic fields, and the Hall conductance terms in $\Pi_\uparrow$ and $\Pi_\downarrow$ will have opposite signs. As shown by Wiegmann[70] in a generic situation, due to the same amplitude but opposite signs of the Hall conductances, K_s in Eq. (2.53) must exhibit the "Meissner effect" in the transverse channel: i.e., $K_s^\perp = 1/4\pi\lambda^2 \neq 0$ at $\omega = 0$ and the $\mathbf{q}\to 0$ limit. Here we find $1/\lambda^2 = \pi B_h J_s$. Such a "Meissner effect" implies that the gauge field will get suppressed in the spinon system. In the long-wavelength and low-energy limit, K_s becomes dominant in the transverse channel of D^a as $K_h \sim 0$, and a nonzero $K_s^\perp$ then leads to a gap $\propto \delta J$ in the transverse gauge fluctuation (2.51) (Anderson-Higgs mechanism). This gap means a spin-charge deconfinement as pointed out before. In contrast, a finite K_s^{-1} will play a *negligible* role in the electromagnetic response function K_e in Eq. (2.50) at small $\mathbf{q}$ and ω, and one finds

$$K_e \simeq K_h, \quad (2.54)$$

in such a limit. So the holon degree of freedom solely determines the long-wavelength, low-energy response to an external electromagnetic field in this spin-charge separation system. Obviously, all these features will disappear at $\delta\to 0$ as B_h vanishes.

The above conclusion is still true if one includes the δA^h dynamics by adding a term $\frac{1}{2}\delta A^h D^{A^{-1}}\delta A^h$ in Eq. (2.52). Here D^A is the free propagator for δA^h which is related to holon density fluctuation as follows:

$$D^A_{\mu\nu} = \left(\delta_{\mu\nu}-\frac{q_\mu q_\nu}{q^2}\right)\left(\frac{\pi^2}{q^2}D^h_\rho\right), \quad (2.55)$$

with D^h_ρ as the holon density-density correlation function. Then Eq. (2.53) is modified as

$$K_s = \left[(\Pi_\uparrow + D^{A^{-1}})^{-1}+\Pi_\downarrow^{-1}\right]^{-1} + \left[\Pi_\uparrow^{-1}+(\Pi_\downarrow+D^{A^{-1}})^{-1}\right]^{-1} + \left[\Pi_\uparrow^{-1}+\Pi_\downarrow^{-1}+\Pi_\uparrow^{-1}(D^A)^{-1}\Pi_\downarrow^{-1}\right]^{-1} + \left[\Pi_\uparrow^{-1}+\Pi_\downarrow^{-1}+\Pi_\downarrow^{-1}(D^A)^{-1}\Pi_\uparrow^{-1}\right]^{-1}. \quad (2.56)$$

Since D^A does not have a transverse-longitudinal mixed term (the Hall term), the above conclusion about K_s can be easily found to remain unchanged as long as D^A approaches a constant or vanishes slower than q^2 when $q\to 0$. (Note that the density-density correlation function[80] of a hard-core boson gas is very similar to a free-fermion gas, and in the latter case one has $D^h_\rho \sim$ const at $\omega = 0$ and $q\to 0$.)

III. SPIN DYNAMICS AT FINITE DOPING

Spin dynamics in the insulating cuprates has been well understood within the framework[50] of the Heisenberg model. A real important issue is how the antiferromagnet is affected under doping. In this section, we will explore such a doping effect under the spin-charge separation scheme, and compare its unique features with those found in the cuprates. We first consider the 1D case, where exact analytical results are available for comparison.

A. Spin-spin correlation in one dimension

The present case corresponds to the large-U limit of the Hubbard model, whose exact solution[52] was obtained a long time ago. However, only recently have the underlying physics and various correlation functions been clarified, following Anderson[32,41] and other authors.[40,45,46,42]

The spin-spin correlation function is one of important correlation functions in 1D. According to a numerical calculation[40] based on the exact solution, a $2k_f$ oscillation is present in the spin-spin correlation function. One may naively relate this incommensurate structure with the existence of a large electron Fermi surface (points at k_f and $-k_f$). A similar argument may also be applied to the 2D case. This observation should be physically reasonable, but by itself is not sufficient to get the correct spin dynamics. Many rich effects will be involved here due to strong electron-electron correlations. In fact, one has a spin-charge separation. In this case, the spinons are presumably responsible for the spin dynamics. But at the same time, holons as solitons of doped holes bound with spin domain walls will also contribute to spin properties. A combination of these decides a peculiar doped spin-spin correlation, which is highly nontrivial from a Fermi-liquid point of view. In the following, we will show how a correct spin-spin correlation can be obtained without directly involving the electron Fermi surface.

In the present scheme, the spin-flip operator S_i^+ in Eq. (2.46) can be expressed in 1D in terms of Eq. (2.20) as

$$S_i^+ = (-1)^i b_{i\uparrow}^\dagger b_{i\downarrow} e^{\pm i\pi \sum_{l>i} n_l^h}. \quad (3.1)$$

Here a prominent feature is a Jordan-Wigner-type nonlocal phase $\pi \sum_{l>i} n_l^h$ which involves the holon number operator. At first glimpse, it may seem strange for a holon number operator to appear in a spin expression. But this is not new, and has already been found in Ref. 42 by a path-integral approach, as a result of spin-charge separation. It actually describes the effect of spin domain walls carried by holons mentioned above. This is easy to see if one freezes the dynamics of spinon $b_{i\sigma}$ by letting it "condense" in Eq. (3.1). Then one would have a Néel order in the spin x-y plane when holons are absent. For each added holon at l site, one finds an extra sign $e^{\pm i\pi} = -1$ for every S_i^+ at $i < l$, which means a flip for all those spins. In other words, there is indeed a spin domain wall accompanying each doped hole, and that is the physical reason why the holon number operator enters into Eq. (3.1) nonlocally. We note that the nonlocal field appearing in Eq. (3.1) can be also related to the phase-shift field that leads to the Luttinger-liquid behavior and an electron Fermi surface satisfying the Luttinger-liquid theorem in the single-electron propagator, which is to be discussed elsewhere. In fact, a $2k_f$ oscillation in the spin correlation function will arise naturally due to this nonlocal field as shown below.

Due to $A_{ij}^s = A_{ij}^h = 0$ in 1D, holons and spinons are decoupled in the Hamiltonians (1.2) and (1.3). The nonlocal phase in Eq. (3.1) will then solely determine the doping effect. One may write

$$\langle S_i^+(t) S_j^-(0)\rangle = (-1)^{i-j} \langle b_{i\uparrow}^\dagger(t) b_{j\uparrow}(0)\rangle \langle b_{j\downarrow}(t) b_{j\downarrow}^\dagger(0)\rangle \langle e^{\pm i\pi \sum_{l>i} n_l^h(t)} e^{\mp i\pi \sum_{l>j} n_l^h(0)}\rangle. \quad (3.2)$$

Since $b_{i\sigma}$ and h_i as described by Eqs. (1.2) and (1.3) are hard-core bosons, each average on the right-hand side of Eq. (3.2) can be evaluated straightforwardly in the asymptotic limit (see Sec. II B, and Ref. 42). For example,

$$\langle e^{\pm i\pi \sum_{l>i} n_l^h(t)} e^{\mp i\pi \sum_{l>j} n_l^h(0)}\rangle \propto \frac{\cos(\frac{\pi}{2a}\delta x)}{(x^2 - v_h^2 t^2)^{1/4}}, \quad (3.3)$$

with $x = x_i - x_j$ and $v_h = 2t_h a \sin(\pi\delta)$. The final result is

$$\langle S_i^+(t) S_j^-(0)\rangle \propto \frac{\cos(2k_f x)}{(x^2 - v_s^2 t^2)^{1/2}(x^2 - v_h^2 t^2)^{1/4}}, \quad (3.4)$$

where $k_f = (1-\delta)\pi/2a$. The doping effect as described by the phase shift in Eq. (3.1) enters Eq. (3.4) by changing the oscillation from $2\pi/a$ to the incommensurate $2k_f$, and at the same time contributing an additional power $(x^2 - v_h^2 t^2)^{-1/4}$. It is noted that $\langle S_i^z(t) S_j^z(0)\rangle$ cannot be directly computed at the same level of approximation as explained in Sec. II, but it should follow the same behavior due to rotational invariance.

Equation (3.4) recovers the correct spin behavior at the strong-coupling fixed point of the model (i.e., the large-U Hubbard model). It suggests that the present state indeed catches the correct characteristics of charge-spin separation in 1D, even though such a scheme was originally constructed for 2D.

B. Doping effect in two dimensions

In the one-dimensional case, spinons and holons are decoupled, and the doping effect on spin dynamics is solely contributed by the spin domain walls carried by holons. In 2D, this nonlocal doping effect takes a different form, because spinons and holons will no longer behave like free solitons. As noted before, the topological phase A_{ij}^h in H_s cannot be gauged away in 2D, and it will represent a new type of nonlocal influence of doping on spinons.

1. New length and energy scales introduced by doping

As shown in Sec. II, the gauge fields confining spinons and holons are suppressed at finite doping. But there are still residual interactions between spinons and holons, and spinons can always feel the existence of holons nonlocally by seeing the flux quanta bound to the latter.

Let us first see how this exotic interaction can change the topology of a holon. In the spin-flip operator S_i^+ [Eq. (2.46)], one has a nonlocal phase $[\sum_{l\neq i} \mathrm{Im} \ln (z_i - z_l) n_l^h]$ involving the holon number operator. Similarly to the domain-wall picture in 1D, one may interpret it as describing a spin vortex in the x-y plane with vorticity 2π bound to each holon. This could be seen if one freezes the dynamics of $b_{i\sigma}^\dagger$ and treats it as a number in Eq. (2.46). But $b_{i\sigma}^\dagger$ here can no longer be regarded as a constant quantity because it is under the topological phase A_{ij}^h in H_s. A Berry-phase counting shows that the phase in $b_{i\sigma}^\dagger$ cancels out the effect of the nonlocal phase shift in Eq. (2.46) such that there is actually no 2π-vortex topological texture formed around a holon. Nevertheless, if one goes along a line *across* such a holon, one can still find a domain-wall-like spin singularity at a holon site similar to that in 1D. Thus, a holon in 2D is no longer associated with a spin topological object. Instead, it may carry a Shraiman-Siggia-type[81] dipolar texture with vorticity $= 0$. Such an object will not break the T and P symmetries. One expects a strong dynamical renormalization to be involved in determining the profile of each holon. However, we are not interested in the single-doped-hole problem here. We shall focus on a finite doping concentration in the following, where a useful mathematical description becomes available.

For simplicity, we are going to use a continuum ver-

sion of the spinon Hamiltonian H_s by taking the lattice constant $a \to 0$. This continuum approximation may be justified at small doping and in the low-energy, long-wavelength regime, where the amplitude of A^h_{ij} is small and the spinons as bosons mainly stay near the bottom of the energy band. Such a continuum version for H_s in Eq. (1.2) can be easily written as (cf. Ref. 68)

$$\tilde{H}_s = \sum_\sigma \int d^2\mathbf{r}\ \ b^\dagger_\sigma(\mathbf{r}) \frac{(-i\nabla - \sigma \mathbf{A}^h)^2}{2m_s} b_\sigma(\mathbf{r}), \tag{3.5}$$

with $m_s = (2J_s a^2)^{-1}$ and $\mathbf{A}^h(\mathbf{r})$ defined by

$$\mathbf{A}^h(\mathbf{r}) = \frac{1}{2}\int d^2\mathbf{r}' \frac{\hat{\mathbf{z}} \times (\mathbf{r} - \mathbf{r}')}{|\mathbf{r} - \mathbf{r}'|^2} \rho_h(\mathbf{r}'). \tag{3.6}$$

Here $\rho_h(\mathbf{r})$ is the holon density, $\rho_h = h^\dagger(\mathbf{r})h(\mathbf{r})$.

We note that Eqs. (3.5) and (3.6) would describe a semion problem[67] if the holon density $\rho_h(\mathbf{r}')$ were replaced by the spinon density. The mathematical similarity suggests that one may borrow the method developed in the anyon problem.[67,82,83] The idea is to rewrite $\rho_h = \bar{\rho_h} + (\rho_h - \bar{\rho_h})$ in Eq. (3.6) by introducing an average holon density $\bar{\rho_h} = \delta/a^2$. Then $\mathbf{A}^h(\mathbf{r})$ is rewritten as

$$\mathbf{A}^h(\mathbf{r}) = \bar{\mathbf{A}}^h(\mathbf{r}) + \delta\mathbf{A}^h(\mathbf{r}) \ . \tag{3.7}$$

Here $\bar{\mathbf{A}}^h(r)$ corresponds to $\bar{\rho}_h$, and in the symmetric gauge it may be expressed by[82,83] $\bar{\mathbf{A}}^h(r) = \frac{B_h}{2}(\hat{\mathbf{z}} \times \mathbf{r})$ with $B_h = \pi\bar{\rho_h}$. Physically, the vector potential $\bar{\mathbf{A}}^h$ describes a mean-field magnetic field B_h obtained after the flux quanta bound to holons are uniformly smeared out in space. $\delta\mathbf{A}^h(\mathbf{r})$ in Eq. (3.7) is the fluctuation part,

$$\delta\mathbf{A}^h(\mathbf{r}) = \frac{1}{2}\int d^2\mathbf{r}' \frac{\hat{\mathbf{z}} \times (\mathbf{r} - \mathbf{r}')}{|\mathbf{r} - \mathbf{r}'|^2} [\rho_h(\mathbf{r}') - \bar{\rho_h}], \tag{3.8}$$

which can be treated perturbatively. We emphasize that in an anyon problem, $\delta\mathbf{A}^h$ would correlate with anyon density fluctuation and represent[82,83] a long-range interaction among anyons. Here $\delta\mathbf{A}^h$ is determined by the density fluctuation of *holons* instead of spinons themselves, which belong to an independent degree of freedom. Thus one expects $\delta\mathbf{A}^h(\mathbf{r})$ to provide an independent dynamical scattering source in Eq. (3.5) just like phonons in a usual electron system.

The separation (3.7) is meaningful when the hole density is not too low. With the presence of a fictitious magnetic field B_h, a new length scale is introduced to the spinon system, which is the magnetic cyclotron length

$$l_c = \frac{1}{\sqrt{B_h}} = \frac{a}{\sqrt{\pi\delta}}. \tag{3.9}$$

l_c will later be connected to the antiferromagnetic correlation length. At this mean-field level, a Landau-level structure appears in the spinon energy spectrum, and a basic energy scale is the cyclotron energy

$$\omega_c = \frac{B_h}{m_s} = 2\pi\delta J_s. \tag{3.10}$$

Another energy scale measuring the broadening Γ_s of each Landau level caused by the fluctuation $\delta\mathbf{A}^h$ should be also correlated with the doping concentration. Γ_s will be related to an important low-energy scale in spin dynamics. It can be estimated to be of an order of magnitude $\sim \delta J$ if the energy scale of the fluctuating $\delta\mathbf{A}^h$ is sufficiently small. Γ_s could be even sharper when the fluctuating $\delta\mathbf{A}^h$ has a higher-energy scale as holons become more mobile at finite doping. Of course, different Landau levels generally could have different broadening widths, and a further discussion will be given later. A similar broadening problem in a semion system has been recently studied by Levy and Laughlin,[84] where the dynamics of $\delta\mathbf{A}^h$ is already known from random-phase-approximation (RPA) calculations. In the present case, the dynamics of $\delta\mathbf{A}^h$ is directly related to that of $\delta\rho_h = \rho_h - \bar{\rho}_h$, which will be in turn determined by coupling with the spinon degree of freedom. So a self-consistent treatment of the Landau-level broadening could be very complicated here. Nevertheless, for the purpose of understanding the basic characteristics for spin dynamics, only a general shape of the Landau-level broadening is needed, and a detailed structure will not be crucial.

Besides the length and energy scales, we point out that there also exists a basic temperature scale which is related to the Bose-condensation temperature T_c^* of the bosonic spinon $b_{i\sigma}$. Recall that for a 2D free-boson gas, a 2D Bose condensation is always suppressed by the thermal excitations at any finite temperature, due to a finite density of states at low energy. In the present case, due to the broadening of the lowest Landau level (LLL), the low-energy density of states presumably will fall off continuously to zero at the LLL energy bottom. Thus the low-lying thermal excitation has vanishing weight at the low-energy tail, which could not halt the Bose condensation of spinons at a sufficiently low temperature. As will be demonstrated later, T_c^* will represent an important temperature scale in spin dynamics.

2. *Spin susceptibility function*

The spin dynamic structure factor $S(\mathbf{q}, \omega)$ is defined as a Fourier transformation of the spin-spin correlation function

$$S_{\alpha\beta}(\mathbf{q}, \omega) = \frac{1}{2\pi}\int_{-\infty}^{\infty} dt e^{i\omega t} \int d^2\mathbf{r} e^{-i\mathbf{q}\cdot\mathbf{r}} \langle \mathbf{S}_\alpha(\mathbf{r}, t) \cdot \mathbf{S}_\beta(0, 0)\rangle. \tag{3.11}$$

$S_{\alpha\beta}(\mathbf{q}, \omega)$ can be directly measured in neutron-scattering experiments, and is related to the dynamic spin susceptibility function $\chi_{\alpha\beta}(\mathbf{q}, \omega)$ through the so-called fluctuation-dissipation theorem,

$$S_{\alpha\beta}(\mathbf{q},\omega)=\frac{1}{\pi}\left[1-e^{-\beta\omega}\right]^{-1}\chi''_{\alpha\beta}(\mathbf{q},\omega), \tag{3.12}$$

where $\beta=1/k_BT$ and $\chi''_{\alpha\beta}(q,\omega)\equiv \mathrm{Im}\chi_{\alpha\beta}(\mathbf{q},\omega+i0^+)$ is the imaginary part of the retarded spin susceptibility function.

In the Matsubara representation, the transverse spin susceptibility is defined by

$$\chi(\mathbf{q},i\omega_n)=\int_0^\beta d\tau e^{i\omega_n\tau}\int d^2\mathbf{r}e^{-i\mathbf{q}\cdot\mathbf{r}}\langle T_\tau S^+(\mathbf{r},\tau)S^-(0,0)\rangle, \tag{3.13}$$

with $\omega_n=2\pi n/\beta$. In terms of a continuum version of Eq. (2.46), one may write

$$\langle T_\tau S^+(\mathbf{r},\tau)S^-(0,0)\rangle=\frac{a^2}{4}\left(\sum_{\mathbf{Q}_0}e^{i\mathbf{Q}_0\cdot\mathbf{r}}\right)\langle T_\tau b^\dagger_\uparrow(\mathbf{r},\tau)b_\uparrow(0,0)e^{i\int_{(0,0)}^{(\mathbf{r},\tau)}\mathbf{A}^h\cdot d\mathbf{r}}\rangle\langle T_\tau b_\downarrow(\mathbf{r},\tau)b^\dagger_\downarrow(0,0)e^{-i\int_{(\mathbf{r},\tau)}^{(0,0)}\mathbf{A}^h\cdot d\mathbf{r}}\rangle, \tag{3.14}$$

in which $\mathbf{Q}_0=(\pm\frac{\pi}{a},\pm\frac{\pi}{a})$ are the AF wave vectors. $\mathbf{A}^h$ in Eq. (3.14) is from the nonlocal phase in the spin expression (2.46). In the mean-field approximation with $\mathbf{A}^h$ replaced by $\bar{\mathbf{A}}^h$, Eq. (3.14) may be rewritten as

$$\langle T_\tau S^+(\mathbf{r},\tau)S^-(0,0)\rangle=\frac{a^2}{4}\left(\sum_{\mathbf{Q}_0}e^{i\mathbf{Q}_0\cdot\mathbf{r}}\right)e^{2i\int_0^{\mathbf{r}}\bar{\mathbf{A}}^h\cdot d\mathbf{r}}G^\uparrow_b(-\mathbf{r},-\tau)G^\downarrow_b(\mathbf{r},\tau), \tag{3.15}$$

where the line integration on the right-hand side is chosen along a straight line connecting (x,y) and $(0,0)$ on the 2D plane. The Green's function G^σ_b is defined by

$$G^\sigma_b(\mathbf{r},\tau)=-\langle T_\tau b_\sigma(\mathbf{r},\tau)b^\dagger_\sigma(0,0)\rangle. \tag{3.16}$$

$b_\sigma(\mathbf{r})$ may be expressed in the representation of the Landau levels as $b_\sigma(\mathbf{r})=\sum_{nk}\langle\mathbf{r}|nk\rangle b^\sigma_{nk}$, where $n=0,1,2,\ldots$ is the Landau-level index and k is the quantum number inside each Landau level. Correspondingly,

$$\begin{aligned}G^\sigma(\mathbf{r},\tau)&=-\sum_{n,k}\sum_{n',k'}\langle\mathbf{r}|nk\rangle\langle n'k'|\mathbf{0}\rangle\langle T_\tau b^\sigma_{nk}(\tau)(b^\sigma_{n'k'})^\dagger(0)\rangle\\&=-\sum_n\left\langle\mathbf{r}\left|\left(\sum_k|nk\rangle\langle nk|\right)\right|0\right\rangle\langle T_\tau b^\sigma_{nk}(\tau)(b^\sigma_{nk})^\dagger(0)\rangle\\&=\sum_n\Pi^\sigma_n(\mathbf{r},\mathbf{0})G^\sigma_b(n,\tau).\end{aligned} \tag{3.17}$$

In obtaining last line of Eq. (3.17), the k dependence of the Green's function $G_b=-\langle T_\tau b_{nk}(\tau)b^\dagger_{nk}(0)\rangle$ has been neglected. Note that k represents the center of each cyclotron orbital in the present symmetric gauge and the k dependence of G_b should not be important due to the translational invariance of the system. $\Pi^\sigma_n(\mathbf{r},\mathbf{0})$ in Eq. (3.17) is given by[82]

$$\Pi^\sigma_n(\mathbf{r},0)=L_n\left(\frac{r^2}{2l_c^2}\right)\Pi^\sigma_0(\mathbf{r},\mathbf{0}), \tag{3.18}$$

with $L_n(t)$ as the Laguerre polynomials, $L_0(t)=1$, $L_1(t)=1-t$, etc., and

$$\Pi^\sigma_0(\mathbf{r},\mathbf{0})=\frac{1}{2\pi l_c^2}\exp\left[-r^2/4l_c^2\right]. \tag{3.19}$$

Then one gets

$$\chi(\mathbf{q},i\omega_n)=\sum_{l,m=0}^{\infty}K_{lm}(\mathbf{q})\int_{-\infty}^{\infty}\frac{d\omega'd\omega''}{2\pi}\rho_b(l,\omega')\rho_b(m,\omega'')\frac{n(\omega'')-n(\omega')}{i\omega_n+\omega'-\omega''}, \tag{3.20}$$

where

$$\begin{aligned}K_{lm}(\mathbf{q})&=\frac{a^2}{32\pi^3l_c^4}\sum_{\mathbf{Q}_0}\int d^2\mathbf{r}L_l\left(\frac{r^2}{2l_c^2}\right)L_m\left(\frac{r^2}{2l_c^2}\right)e^{-\frac{r^2}{2l_c^2}}e^{-i\mathbf{r}\cdot(\mathbf{q}-\mathbf{Q}_0)}\\&=\frac{\delta}{16\pi}\sum_{\mathbf{Q}_0}\int_0^\infty dyL_l(y)L_m(y)e^{-y}J_0(\sqrt{2l_c^2y}\,|\mathbf{q}-\mathbf{Q}_0|),\end{aligned} \tag{3.21}$$

with $J_0(x)$ as the Bessel function, and the spectral function ρ_b is defined through

$$G_b^\sigma(l, i\omega_n) = \int \frac{d\omega'}{2\pi} \frac{\rho_b(l,\omega')}{i\omega_n - \omega'}, \tag{3.22}$$

in which the spin index σ has been omitted for simplicity since ρ_b does not explicitly depend on it in the unpolarized case. $n(\omega) = 1/(e^{\beta\omega}-1)$ in Eq. (3.20) is the Bose distribution function. Note that the spectral function $\rho_b(l,\omega)$ ensures $\omega \geq \omega_0 - \mu \geq 0$, where ω_0 is the energy minimum of spinon spectrum and μ is the chemical potential determined by $\sum_l (2\pi l_c^2)^{-1} \int (d\omega/2\pi)\rho(l,\omega)n(\omega) = (1-\delta)/2a^2$.

Finally $\chi''(\mathbf{q},\omega)$ is found by

$$\chi''(\mathbf{q},\omega) = -\pi \sum_{l,l'} K_{ll'}(\mathbf{q}) \int_{-\infty}^{\infty} \frac{d\omega'}{2\pi} \rho_b(l,\omega')\rho_b(l',\omega+\omega') \left[n(\omega+\omega') - n(\omega')\right]. \tag{3.23}$$

In the next sections, we shall examine the $\mathbf{q}$ dependence, ω dependence, and temperature dependence of $\chi''(\mathbf{q},\omega)$ and compare them with neutron-scattering and NMR experimental measurements in cuprates.

3. Basic characteristics of spin dynamics in 2D

The spin susceptibility $\chi''(\mathbf{q},\omega)$ in Eq. (3.23) will characterize the basic features of the spin dynamics. The real part of the spin susceptibility can be also determined from $\chi''(\mathbf{q},\omega)$ through the Kramers-Kronig relation. Here we shall mainly focus on $\chi''(\mathbf{q},\omega)$ in the vicinity of the AF wave vector $\mathbf{Q}_0$ and low energy ω.

As discussed in Sec. I, doping creates a Landau-level structure in the spinon spectrum. So low-lying spin fluctuations are expected to be sensitive to doping. Due to the particular Landau-level structure, one can distinguish two types of contributions to $\chi''(\mathbf{q},\omega)$, which correspond to an intra-Landau-level transition and an inter-Landau-level transition, respectively. We will show below that these two processes are related to the so-called commensurate and incommensurate AF spin fluctuations in the present state.

Commensurate AF fluctuation. First we consider $\chi''(\mathbf{q},\omega)$ at small ω such that only the intra-Landau-level transition contributes. At low temperature with spinons staying in the LLL, the $\mathbf{q}$ dependence of $\chi''(\mathbf{q},\omega)$ [Eq. (3.23)] is solely decided by $K_{00}(\mathbf{q})$:

$$K_{00}(\mathbf{q}) = \frac{\delta}{16\pi} \sum_{\mathbf{Q}_0} \exp\left(-\frac{|\mathbf{q}-\mathbf{Q}_0|^2}{2l_c^{-2}}\right), \tag{3.24}$$

in terms of Eq. (3.21). Equation (3.24) shows that $\chi''(\mathbf{q},\omega)$ will be peaked at the AF wave vector $\mathbf{Q}_0$'s. The corresponding spin fluctuation is known as the commensurate AF fluctuation. With the increase of temperature, spinons can be thermally excited to higher Landau levels such that $K_{11}(\mathbf{q})$, $K_{22}(\mathbf{q})$, etc., will contribute. For example, $K_{11}(\mathbf{q})$ has the following form:

$$K_{11}(\mathbf{q}) = \frac{\delta}{16\pi} \sum_{\mathbf{Q}_0} \left(1 - \frac{|\mathbf{q}-\mathbf{Q}_0|^2}{2l_c^{-2}}\right)^2 \exp\left(-\frac{|\mathbf{q}-\mathbf{Q}_0|^2}{2l_c^{-2}}\right), \tag{3.25}$$

which is still peaked at $\mathbf{Q}_0$ with a width essentially the same as $K_{00}(\mathbf{q})$ in Eq. (3.24). K_{ll} at higher l can be checked by numerical calculation and generally a Gaussian (3.24) is well satisfied when l is not too large. This means that the width is not sensitive to temperature.

Thus, when the intralevel transition dominates, $\chi''(\mathbf{q},\omega)$ generally follows a Gaussian:

$$\chi''(\mathbf{q},\omega) \simeq \exp\left(-\frac{|\mathbf{q}-\mathbf{Q}_0|^2}{(2\sigma^2)}\right) A(\omega), \tag{3.26}$$

around $\mathbf{Q}_0$, where $\sigma = 1/l_c$ and $A(\omega) \equiv \chi''(\mathbf{Q}_0,\omega)$. The Gaussian (3.26) with a width σ determines the spin-spin correlation in real space: $\cos(\mathbf{Q}_0\cdot\mathbf{r})\exp[-|\mathbf{r}|^2/\xi^2]$, where the correlation length

$$\xi = \frac{\sqrt{2}}{\sigma} = a\sqrt{\frac{2}{\pi\delta}} \tag{3.27}$$

is in the same order of the average hole-hole distance. Namely, the doped holes break up the long-range AF correlation into short-range AF fragments with a length scale $\sim \xi$.

The energy scale of this AF fluctuation will be characterized by the ω dependence of $A(\omega) = \chi''(\mathbf{Q}_0,\omega)$ in Eq. (3.26). Since only the intralevel transition is involved here, the magnetic energy scale will be basically decided by the broadenings of the Landau levels. The expression of $\chi''(\mathbf{Q}_0,\omega)$ can be found as

$$\chi''(\mathbf{Q}_0,\omega) = -\frac{\delta}{16} \int \frac{d\omega'}{2\pi} \sum_l \rho_b(l,\omega')\rho_b(l,\omega+\omega') \left[n(\omega+\omega') - n(\omega')\right]. \tag{3.28}$$

Here the broadening width Γ_s of the spectral function ρ_b for a given Landau level is generally of the order δJ, as caused by the fluctuation $\delta \mathbf{A}_h$. The detailed broadenings will be sensitive to $\delta \mathbf{A}_h$ and other factors, which is to be further discussed later. Equation (3.28) has been obtained from Eq. (3.23) by using

$$K_{ll'}(\mathbf{Q}_0) = \frac{\delta}{16\pi}\delta_{l,l'}, \tag{3.29}$$

in terms of Eq. (3.21) and the orthogonality of the Laguerre functions,

$$\int_0^\infty dy L_l(y) L_{l'}(y) e^{-y} = \delta_{l,l'}. \tag{3.30}$$

[The contribution to $K_{ll'}(\mathbf{Q}_0)$ from the other three $\mathbf{Q}_0$'s is exponentially small and has been neglected.]

The typical ω dependence of $\chi''(\mathbf{Q}_0,\omega)$ is shown in Fig. 1 at various temperatures. The choice of the spectral function ρ_b and other parameters in Fig. 1 is to describe the underdoped $YBa_2Cu_3O_{6.6}$, which will be explained in the next section. Here we mainly focus on the general features shown in Fig. 1. Besides an overall small energy scale decided by the Landau-level broadening, Fig. 1 shows an interesting temperature effect characterized by the Bose-condensation temperature T_c^*. When $T > T_c^*$, one finds $\chi''(\mathbf{Q}_0,\omega) \propto \omega/T$ at small ω. The slope of the linear ω dependence *increases* with the decrease of T. However, this *increase* gets arrested at $T = T_c^*$, and when $T < T_c^*$ the low-energy part of $\chi''(\mathbf{Q}_0,\omega)$ becomes continuously suppressed instead. This feature resembles a typical "spin-gap" behavior. When $T < T_c^*$, the spinons begin to condensate into the bottom state of the lowest Landau level. The contribution due to the transition from such a condensate state to the rest of the quantum states in the broadened LLL will then emerge in $\chi''(\mathbf{Q}_0,\omega)$. This process effectively will map out the shape of the spectral function of the same Landau level, and becomes dominant with the decrease of temperature. In fact, at $T = 0$ when all the spinons are condensed, $\chi''(\mathbf{Q}_0,\omega)$ in Eq. (3.28) is simply reduced to

$$\chi''(\mathbf{Q}_0,\omega)_{T=0} = \left(\frac{n_s}{16}\right)\rho_b(l=0,\omega)_{T=0}, \tag{3.31}$$

with $n_s = 1-\delta$, which is directly proportional to the spectral function $\rho_b(0,\omega)$ of the LLL. If $\rho_b(0,\omega)$ has a small Lifshitz tail before it vanishes at the low-energy end $\omega = 0$, a gap feature is exhibited in $\chi''(\mathbf{Q}_0,\omega)$ as illustrated in Fig. 1. Even in the case that $\rho_b(0,\omega)$ does not approach to zero very fast at $\omega = 0$, $\chi''(\mathbf{Q}_0,\omega)$ could still generically show a pseudogap trend below $T < T_c^*$ as described above. This spin-gap behavior and the temperature scale T_c^* are the unique and important features of the present spin state.

Another interesting property of $\chi''(\mathbf{q},\omega)$ is its behavior at $\omega \to 0$ limit. This behavior can be probed by NMR measurements.[8] The NMR spin-lattice relaxation rate of nuclear spin due to the coupling to spin fluctuation described by $\chi''(\mathbf{q},\omega)$ is given by[85]

$$\frac{1}{T_1} = \frac{k_B T}{N}\sum_{\mathbf{q}} A^2(\mathbf{q})\frac{\chi''(\mathbf{q},\omega)}{\omega}\bigg|_{\omega\to 0}, \tag{3.32}$$

where the form factor $A^2(\mathbf{q})$ is from the hyperfine coupling between nuclear spin and the spin fluctuation. For $^{63}Cu(2)$ nuclear spin in the cuprates, with the applied field perpendicular to the CuO_2 plane, the form factor $A^2(\mathbf{q})$ is found to be[11,12,14]

$$A^2(\mathbf{q})\big|_{^{63}Cu} = [A_\perp + 2B(\cos q_x a + \cos q_y a)]^2, \tag{3.33}$$

where the hyperfine couplings $A_\perp$ and B are estimated as[14] $A_\perp/B \simeq 0.84$, $B \simeq 3.8\times 10^{-4}$ meV (these coefficients may slightly vary among YBCO and LSCO compounds). For $^{17}O(2)$ nuclear spin, one has[11,12,14]

$$A^2(\mathbf{q})\big|_{^{17}O} = 2C^2[1+\cos(q_x a)], \tag{3.34}$$

with $C \simeq 0.87B$.[14] $A^2(\mathbf{q})|_{^{17}O}$ in Eq. (3.34) vanishes at $\mathbf{q} = \mathbf{Q}_0$. Thus a combined measurement of $1/^{63}T_1$ and $1/^{17}T_1$ can provide $\mathbf{q}$-dependent information about $\chi''(\mathbf{q},\omega)$ at $\omega \to 0$.

In the present framework, $\chi''(\mathbf{q},\omega)$ have been already obtained in Eq. (3.23). So by substituting it into the above $1/T_1$ expression, it is straightforward to get

$$\frac{1}{^{63}T_1} = \pi\sum_l C_l \int \frac{d\omega}{2\pi} n(\omega)[1+n(\omega)][\rho_b(l,\omega)]^2, \tag{3.35}$$

where

$$C_l = \frac{\delta^2 B^2}{8\pi}\left[\left(\frac{A_\perp^2}{B^2}+4\right) - 8\frac{A_\perp}{B}L_l^2\left(\frac{a^2}{\xi^2}\right)e^{-a^2/\xi^2} + 8L_l^2\left(\frac{2a^2}{\xi^2}\right)e^{-2a^2/\xi^2} + 4\left(\frac{4a^2}{\xi^2}\right)e^{-4a^2/\xi^2}\right]. \tag{3.36}$$

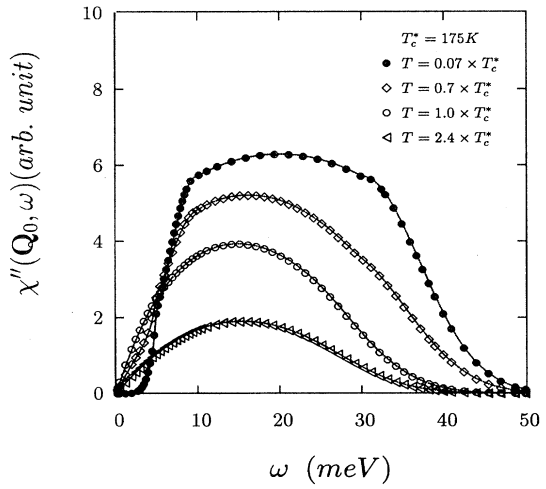

FIG. 1. $\chi''(\mathbf{Q}_0,\omega)$ vs ω. A pseudo-spin-gap behavior is exhibited at $T < T_c^*$, where the low-energy part ($\simeq$ 5 meV) is continuously suppressed with the decrease of the temperature. The spectral function in $\chi''(\mathbf{Q}_0,\omega)$ is chosen to describe $YBa_2Cu_3O_{6.6}$ (see text).

In obtaining Eqs. (3.35) and (3.36) only the intralevel transition (i.e., $l = l'$) is involved. Using the same $\chi''(\mathbf{q},\omega)$ whose ω dependence at $\mathbf{q} = \mathbf{Q}_0$ is illustrated in Fig. 1, one finds the corresponding $1/^{63}T_1T$ vs T as shown in Fig. 2. In contrast to a usual Korringa rule for a Fermi liquid, $1/T_1T \sim$ const, Fig. 2 clearly depicts a non-Korringa behavior which falls off like $\propto 1/T$ at high temperature. And $1/^{63}T_1T$ is peaked at the characteristic temperature T_c^*, below which $\chi''(\mathbf{Q}_0,\omega)$ begins to develop a "spin-gap" behavior.

On the other hand, at the ^{17}O(2) site, the coefficient C_l has to be replaced by $C_l^{\rm O}$ in Eq. (3.35):

$$C_l^{\rm O} = \frac{\delta^2 C^2}{4\pi}\left[1 - L_l^2\left(\frac{a^2}{\xi^2}\right)e^{-a^2/\xi^2}\right]. \tag{3.37}$$

The difference between $1/^{63}T_1$ and $1/^{17}T_1$ is due to the different weight functions [Eqs. (3.33) and (3.34)], which pick up the commensurate magnetic fluctuation around $\mathbf{q} = \mathbf{Q}_0$ at the ^{63}Cu(2) site, but suppresses such a contribution at the ^{17}O(2) site. $C_l^{\rm O}$ in Eq. (3.37) simply vanishes at $\xi \to \infty$: the long-range AF limit where the whole contribution is from $\mathbf{q} = \mathbf{Q}_0$. At $\xi = 4a$, for example, we find a reduction of $\sim 1/93$ for $1/^{17}T_1$ as compared to $1/^{63}T_1$. Thus the commensurate AF fluctuation as described by Eq. (3.26) has a negligible contribution to the spin relaxation for planar oxygen nuclei of the cuprates. In contrast, nonmagnetic incoherent contributions should not be suppressed so strongly by the form factor, and would become the dominant contribution in $1/^{17}T_1$ as well as in the Knight shift,[8] which measures the real part of the spin susceptibility near $\mathbf{q} = 0$.

Hence, $\chi''(\mathbf{q},\omega)/\omega$ at $\omega \to 0$ gives rise to a non-Korringa behavior of the NMR spin relaxation rate. This $1/T$ law of $1/T_1T$ can be obtained analytically, if the broadening Γ_s^0 of the spectral function ρ_b for the LLL is small as compared to temperature. That is, when $\Gamma_s^0 \ll T \ll \omega_c$ (and of course $T > T_c^*$), one has

$$\frac{1}{^{63}T_1T} \simeq \frac{D}{T}, \tag{3.38}$$

in terms of Eq. (3.35), where $D = \pi C_0 n_s/\Gamma_s^0\delta^2$. Next let us consider the case when the temperature is further increased such that more Landau levels are involved. Here we have to assume a general Lorentz-like broadening for each Landau level with $\Gamma_s = 0.4\omega_c \propto \delta$. Then $1/^{63}T_1$ at high temperature is shown in Fig. 3, where the curves become very flat and not sensitive to the doping concentration. This is in contrast to the low-temperature regime, where a strong doping dependence can emerge [in Eq. (3.38), $D \sim 1/\delta$ if one simply takes $\Gamma_s^0 \propto \delta$].

Therefore, a full picture for the low-lying commensurate AF correlation is formed for the present spin-charge separation state. This picture is rather unique, and is drastically different from those of Fermi liquid and local antiferromagnetic descriptions. The doping effect plays a key role here. It decides a doping-dependent energy scale for the AF fluctuation, which can be much smaller than the characteristic energies in a Fermi liquid (ϵ_f) and an effective local antiferromagnet ($[1-\delta]J$). It also leads to a doping-dependent correlation length, comparable with the average spacing of holes. Furthermore, the Bose condensation of spinons determines a new characteristic temperature scale, below which the low-lying spin fluctuation is suppressed and the non-Korringa behavior of the spin relaxation rate gets interrupted, similarly to a spin-gap effect.

Incommensurate AF fluctuation. Now let us consider the higher-energy regime. If ω is increased such that the inter-Landau-level transition gets involved, the simple Gaussian-like $\mathbf{q}$ dependence in Eq. (3.26) will be mod-

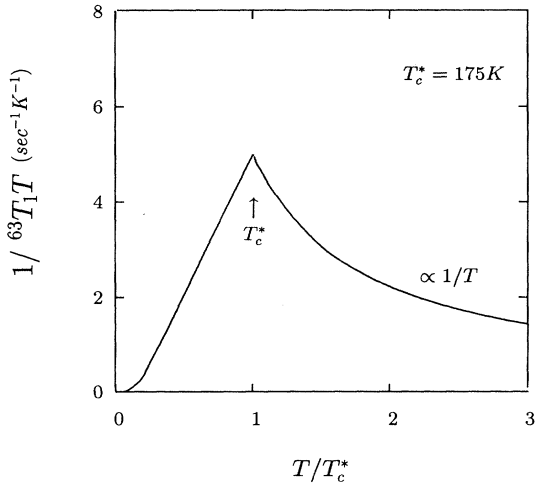

FIG. 2. The NMR spin-lattice relaxation rate for the planar Cu nuclei calculated in terms of the same spectral function used in Fig. 1.

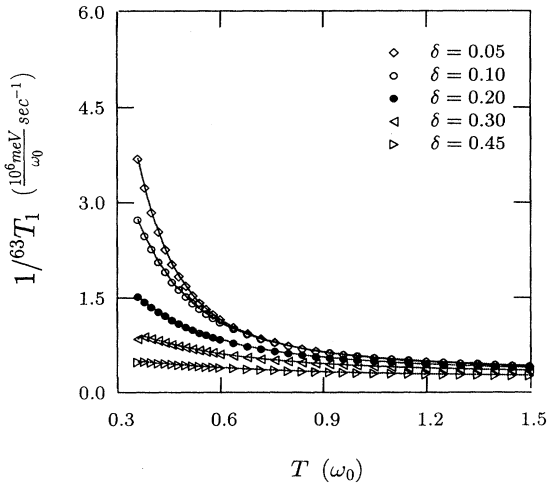

FIG. 3. High-temperature behaviors of the Cu nuclear spin relaxation rate at various doping concentrations. Notice that the spin relaxation rates are leveled off at high temperature and are essentially indistinguishable at small doping ($\delta < 0.2$).

ified. A typical $\chi''(\mathbf{q},\omega)$ vs $\mathbf{q}$ is shown in Fig. 4 at different ω's. For the purpose of illustration, we have chosen the same broadening $\Gamma_s = 0.4\omega_c = 0.4\delta\omega_0$ for each Landau level, and $T = 0.1\omega_0$, $\delta = 0.15$. It shows that the width of the Gaussian is broadened at first with the increase of ω. Then the commensurate peak at $\mathbf{Q}_0$ is split and two incommensurate peaks emerge at some fixed positions as the interlevel transition becomes dominant. In fact, this incommensurate structure is due to $K_{01}(\mathbf{q})$ in Eq. (3.23). According to Eq. (3.21), one finds

$$K_{01}(\mathbf{q}) = \frac{\delta}{16\pi}\sum_{\mathbf{Q}_0}\frac{|\mathbf{q}-\mathbf{Q}_0|^2}{2\sigma^2}\exp\left(-\frac{|\mathbf{q}-\mathbf{Q}_0|^2}{2\sigma^2}\right), \quad (3.39)$$

which leads to incommensurate peaks at a ring circling $\mathbf{Q}_0$ by a radius of $\sqrt{2\pi\delta}/a$. We stress that the doping concentration is presumably small here so that the lattice effect is negligible. At a finite doping where the spin correlation length becomes comparable with the lattice spacing, the lattice effect is expected to become important, which could strongly affect the positions of the incommensurate peaks in $\mathbf{q}$ space. In this case, both flux and lattice have to be treated on the same footing like in the incommensurate flux phase.[69]

With the further increase of ω, a more complicated structure will show up as K_{02}, K_{03}, etc., are involved. The weight of $\chi''(\mathbf{q})$ will be further shifted towards whole Brillouin zone, i.e., the nonmagnetic regime. At such a high energy, the present continuum approximation may no longer be appropriate. Nevertheless, one could still get some generic features. By integrating $\mathbf{q}$ within the whole $\mathbf{q}$ space, we get

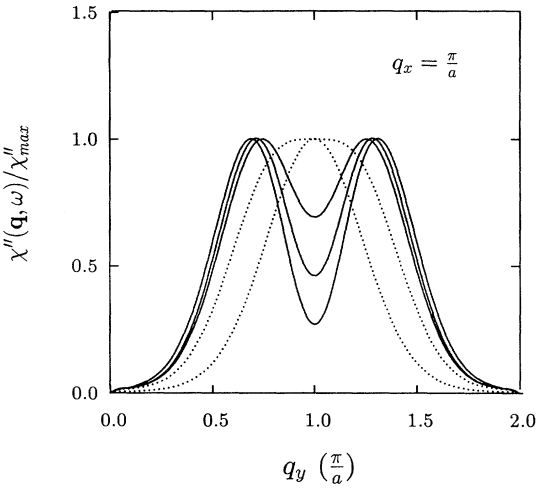

FIG. 4. Typical $\chi''(\mathbf{q},\omega)$ vs $\mathbf{q}$ at various ω's. With the increase of ω, the Gaussian form first gets broadened [dotted curves with $\omega = 0.10$ and 0.15 (ω_0 as the unit)], and then an incommensurate split occurs when the interlevel transition becomes dominant (solid curves with $\omega = 0.18$, 0.20, and 0.30).

$$\chi''_{\text{total}}(\omega) = \frac{1}{N}\sum_{\mathbf{q}}\chi''(\mathbf{q},\omega)$$
$$= \frac{\delta^2}{8\pi}\int\frac{d\omega'}{2\pi}\left[\sum_l \rho_b(l,\omega')\right]\left[\sum_m \rho_b(m,\omega+\omega')\right][n(\omega+\omega')-n(\omega')]. \quad (3.40)$$

Equation (3.40) predicts that at high energy, the $\mathbf{q}$-integrated $\chi''_{\text{total}}(\omega)$ will be saturated at a constant level, modulated by a Landau-level-like oscillation. We note that the higher-energy part is contributed by those fluctuations with less magnetic character. Thus it is less easy for elastic neutron scattering to fully collect data for $\chi''_{\text{total}}(\omega)$. On the other hand, at low energy, finite widths of the Landau levels will lead to a more broadened first peak in $\chi''_{\text{total}}(\omega)$ as compared to the overall energy peak of $\chi''(\mathbf{Q}_0,\omega)$ where only intralevel transitions are involved.

C. Comparison with experimental measurements in cuprates

The normal-state spin dynamics represents an important characteristic for the high-T_c cuprates. Many measurements have been done on these materials, especially YBCO and LSCO compounds. Experimental results have revealed rather rich phenomena, and also seem to suggest that material-dependent effects, like the double-layer structure in YBCO, may play major roles in the spin dynamics. Thus, whether there is an underlying universal mechanism for spin dynamics in the cuprates is not transparent in terms of the experiments alone. In the following, we argue that the present spin-charge separation scheme can relate a variety of anomalous spin properties together, and provide a consistent picture for these materials.

In the underdoped cuprates, like $YBa_2Cu_3O_{6.6}$ and insulating $La_{1.95}Ba_{0.5}CuO_4$, a commensurate AF fluctuation has been verified by neutron scattering,[19,20,17] which is peaked at $\mathbf{Q}_0$ in χ''. These neutron data have been well fitted[20,17] by a Gaussian form (3.26), and the width σ is indeed roughly independent of temperature. The corresponding spin-spin correlation length follows a $a/\sqrt{\delta}$ rule similar to Eq. (3.27), as shown[16] in LSCO at small

doping. Thus the momentum feature of the commensurate AF fluctuation at small doping is well described by the theory. In underdoped $YBa_2Cu_3O_{6+x}$, the energy scale of such a commensurate AF fluctuation has been systematically investigated.[19,86,87] It is found to be doping dependent and small compared to the exchange energy $J \simeq 120$ meV. As discussed in the last section, a small, doping-sensitive energy scale for the commensurate AF fluctuation is one of intrinsic features of the present scheme, and is distinguished from the usual Fermi liquid as well as the local spin descriptions. To our knowledge, so far there is no other alternative theory able to obtain such a small energy scale ($\ll J$) for the commensurate AF fluctuation. Furthermore, a prominent feature has been exhibited[19,20] at the low-energy part of the spectroscopy, where the weight of χ'' is continuously suppressed below some characteristic temperature, resembling an opening of a spin gap. In the present theory, even though there is no real gap in the spin fluctuation spectrum, a characteristic temperature T_c^* is found to be naturally associated with a spin-gap-like phenomenon. In Fig. 1, a typical energy and temperature dependence of $\chi''(\mathbf{Q}_0,\omega)$ has been shown, where the spectral function is chosen to describe $YBa_2Cu_3O_{6.6}$ (see below). And the overall energy and temperature features in Fig. 1, particularly the "spin-gap" behavior, are in good agreement with those found in underdoped $YBa_2Cu_3O_{6+x}$.[19,20] In the underdoped cuprates, the NMR spin relaxation rate of planar copper nuclei[88] manifests a non-Korringa behavior, which is suppressed when the spin-gap feature shows up in neutron scattering at low temperature. In contrast, a conventional Korringa temperature behavior[88] is found for planar oxygen nuclei. The theoretical $1/^{63}T_1T$ has been presented in Fig. 2, which is calculated by using the same spectral function as used in Fig. 1 for $YBa_2Cu_3O_{6+x}$. Figure 2 shows a non-Korringa behavior at $T > T_c^*$ as well as a "spin-gap" feature below T_c^*. All of them are also qualitatively consistent with the experimental measurements [the contribution of the present *commensurate* AF fluctuation to $1/^{17}T_1T$ is dramatically suppressed ($\sim 1/93$ at $\xi \sim 4a$ for $YBa_2Cu_3O_{6.6}$) so that the non-Korringa signal does not leak to the oxygen sites]. Therefore, the $\mathbf{q}$, ω, and T dependences of the present low-lying magnetic fluctuation at small doping are all in agreement with the main experimental features found in the underdoped cuprates.

Let us discuss the spectral function used in the theoretical calculation. According to Eq. (3.31), one may use the experimental measurement of $\chi''(\mathbf{Q}_0,\omega)$ at low temperature to determine $\rho_b(0,\omega)$, instead of a first-principles calculation which would involve much more complicated factors here like interlayer coupling. As $\rho_b(0,\omega)$ satisfies the normalized condition, if its broadening at low temperature is quite large as compared to the temperature scale in which we are interested, the temperature dependence of $\rho_b(0,\omega)$ may not be important. Then $\chi''(\mathbf{Q}_0,\omega)$ in a whole temperature range can be determined. In Fig. 1, we have chosen $\rho_b(0,\omega)$ so as to give the right energy scale of $\chi''(\mathbf{Q}_0,\omega)$ for $YBa_2Cu_3O_{6.6}$ at low temperature (Fig. 7 in Ref. 20). The contribution from the higher Landau levels are neglected because the temperature range considered is comparatively smaller than the broadening of the LLL. Besides the shape of $\rho_b(0,\omega)$, an overall strength of $\chi''(\mathbf{Q}_0,\omega)$ has also been adjusted, in order to compare with experiment, by reducing the spinon concentration from $n_s = 1-\delta$ to $n_s^* < n_s$. This is because in the present approximation the spinons are treated as ideal bosons instead of hard-core bosons. At half-filling, this approximation could lead to a too large magnetization. In the present doped case, it would also give rise to a too strong magnetic fluctuation. The hard-core effect as well as the incoherent band in the spinon spectrum should reduce the effective number of spinons contributing to the AF correlation. We find a reduction of $n_s^*/n_s \sim 1/3$ at $\delta = 0.10$, giving a $T_c^* \simeq 175$ K, consistent with the corresponding experimental characteristic temperature (~ 160 K),[19,20] and *at the same time*, leading to a spin relaxation rate whose magnitude quantitatively agrees with the NMR measurement.[88,8]

To end the discussion of underdoped materials, we give several remarks below. Some authors[89–91] have attributed the spin-gap phenomenon in underdoped YBCO to its peculiar bilayer structure. In contrast, one may have noticed that the theory here is purely two dimensional. Nevertheless, it has been noted that the spinon spectral function $\rho_b(0,\omega)$ for the LLL has been determined directly from experiments, in which the interlayer coupling could have been already included and may play a key role in the broadening. Recall that in the present scheme, there is no real gap opened in the spin spectrum, and the "gap" feature is very sensitive to the detailed broadening of the LLL. Theoretically, for a pure 2D system one would expect the broadening of the LLL to be much narrower at low temperature. The reason is that a spinon in the LLL could not be scattered into a lower-energy state while it emits a phononlike excitation of $\delta\mathbf{A}^h$, because it is already at the energy bottom. It cannot jump up to higher Landau levels either, due to energy conservation. Such a feature has been indeed found in a similar problem.[84] If this were true, the energy scale in the underdoped material might have been much sharper than observed. But in insulating cuprates like $La_{1.95}Ba_{0.5}CuO_4$,[17] holons should be localized and randomly distributed such that $\delta\mathbf{A}^h$ describes a random flux with energy scale $\simeq 0$, instead of a phononlike dynamic mode. Then the degeneracy of the LLL can be lifted under the static random vector potential, and consequently a much broadened LLL could appear. And mixing with other levels is also expected here. For underdoped YBCO, however, one is in the metallic phase, and holes must be mobile which would lead to a well-defined dynamics for $\delta\mathbf{A}^h$. Nonetheless, one may still expect a strong localization tendency of holes at low temperature, as suggested by transport measurements,[1] which could in turn lead to a more broadened LLL than in the optimally doped regime. *Furthermore*, the bilayer coupling in YBCO can split a sharp LLL into two peaks (symmetric and antisymmetric states), but for a larger broadened LLL, the bilayer coupling may well result in a single, much broadened peak like the one shown[20] in $YBa_2Cu_3O_{6.6}$. Finally, we point out that in these underdoped materials, an incommensurate structure has not

been observed yet at high energy. But the width σ in Eq. (3.26) has been found to increase with energy, which is an indication of the involvement of interlevel transition in the present theory.

Next we consider optimally doped cuprates, like $YBa_2Cu_3O_{7-y}$ and metallic $La_{2-x}Sr_xCuO_4$. A striking common feature in these materials is the *lack* of a commensurate AF fluctuation at low energy in neutron measurements. A spin-polarized neutron-scattering measurement[21] of $YBa_2Cu_3O_{7-y}$ has only revealed a sharp high-energy AF peak around 41 meV. In metallic LSCO ($x = 0.075$, 0.14, and 0.15), an incommensurate structure has been found[18] down to an energy scale $\simeq 1$ meV, and no commensurate AF correlation is observed within the experimental resolution. However, the absence of a low-energy AF fluctuation or the presence of a low-energy incommensurate fluctuation would be both in sharp conflict with the NMR measurements[8] which probes the $\omega \simeq 0$ regime and implies strong *commensurate* AF correlations in these materials. For example, by extrapolating the spin susceptibility with the incommensurate structure observed by neutron scattering down to the NMR frequency ($\sim 10^{-4}$ meV), it has been found[22,23] that a large magnetic contribution could leak to $^{17}O(2)$ sites, in contrast to the measured spin relaxation rate $1/^{17}T_1$ which appears[8] to be completely dominated by a nonmagnetic ($\sim$ **q**-independent) contribution. As a matter of fact, the spin relaxation rates in LSCO have shown canonical behaviors, which basically are the same as those found in YBCO compounds. As elaborated in Sec. III B 3, only a commensurate contribution can lead to a non-Korringa behavior of $1/T_1$ at $^{63}Cu(2)$ sites and, *at the same time*, be strongly canceled out at $^{17}O(2)$ sites. This fact has been the basis for the so-called nearly antiferromagnetic-Fermi-liquid theory.[14,92] Therefore, in order to reconcile neutron and NMR experiments, one is led to the conclusion that a commensurate AF fluctuation should reemerge in the optimally doped cuprates within an energy scale beyond the experimental resolution.

However, it is hard to perceive such a characteristic scale in a conventional theory. So far, there have been a number of theoretical conjectures for the mechanism of incommensurate magnetic fluctuations in metallic LSCO. In the Fermi-liquid-like framework, the incommensurability is directly connected[29,27] with the Fermi-surface shape. But it lacks a small energy scale, within which a commensurate structure could be recovered. The spiral state of Shraiman and Siggia[93] based on the t-J model also provides an incommensurate structure. The original spiral state is a long-ranged state, and some short-range versions have been proposed.[94,95] But a low-energy commensurability is still hard to comprehend here. Some nonintrinsic mechanism for the incommensurability due to the inhomogeneity in the LSCO system has been also proposed[23] in order to reconcile the neutron and NMR data, where the commensurate AF fluctuation is assumed to be intrinsic in metallic LSCO. Nevertheless, the details still need to be carried out in order to make a comparison with the experiments.

The present spin-charge separation scheme is unique in having a small characteristic energy scale of the commensurate AF fluctuation, as already discussed in the underdoped case. As pointed out there, an even smaller energy scale could be present at the optimal regime as the LLL broadening becomes sharper when holons are very mobile in this larger doping regime. Due to the narrowness of the energy range, the amplitude of χ'' will be also small due to the cancellation of the Bose functions inside Eq. (3.23) (one has $\chi'' \to 0$ at $\omega/T \to 0$). Therefore, this commensurate AF correlation may well be beyond the experimental resolution to be directly observed by neutron scattering. In $YBa_2Cu_3O_{7-y}$, the bilayer coupling could also split the sharp LLL into two peaks as mentioned before. It then explains the sharp 41-meV AF peak found by neutron scattering[21] as a result of the spinon transition between these two split peaks. On the other hand, such an AF fluctuation can give rise to a non-Korringa law of the NMR spin relaxation rate [Eq. (3.38)], which is consistent with NMR measurements in YBCO and LSCO. Imai *et al.*[30] have measured $1/^{63}T_1$ in the $La_{2-x}Sr_xCu_2O_4$ system up to 900 K. At high temperature, all data ($x = 0$–0.15) seem to converge and saturate to the same temperature-independent value 2700 ± 150 sec^{-1}. The theoretical results shown in Fig. 3 agree well with this tendency. And if we choose, say, $\omega_0 = 1000$ K, we find that the saturation value of $1/^{63}T_1$ is about twice larger than the measured one, which is a reasonable value, considering no adjustment of the spectral function has been made to fit the data.

In our theory, the incommensurate fluctuation in metallic LSCO will be attributed to the dominance of the inter-Landau-level transition in the experimental energy-transfer regime, as discussed in Sec. III B 3. To be consistent with neutron-scattering measurements, the LLL broadening has to be very sharp as explained above, while the second level broadening is relatively larger, which should be centered around $\omega_c \sim 10$ meV in the $x = 0.15$ case. When the temperature is increased such that $k_BT \sim \omega_c$, a large amount of spinons is expected to be thermally excited to the second Landau level. Then in the experimental-observable energy regime, the intralevel transition could emerge again due to a larger broadening in the second Landau level. Correspondingly, the incommensurate structure should be replaced once again by the commensurate peak around $\mathbf{Q}_0$. This has been indeed observed in a neutron-scattering measurement,[18] where a broad commensurate peak is found to reemerge around $T \sim 100$ K.

The characteristic energy scale ω_c of YBCO seems to be several times larger than that of LSCO for some unknown reason. This decides the main distinction of spin dynamics between YBCO and LSCO, in terms of the present theory. In other words, one should expect that at a sufficiently high energy, incommensurate structures could also show up in the YBCO system. Of course, many factors, especially the interlayer coupling, may complicate the details. Due to these incommensurate contributions at high energy, the **q**-integrated susceptibility function χ''_{total} [Eq. (3.40)] will stretch up to an overall energy scale $\sim J_s$ with a roughly constant amplitude (modulated by the oscillation). Such a unique χ''_{total}

behavior is a high-energy prediction of the present theory for the cuprates.

In optimally doped LSCO and YBCO, the spin-gap feature is *absent* in the commensurate spectrum due to the fact that the energy scale is too small. But according to the theory, a pseudogap should be also present in the LSCO compounds below T_c^*, which involves an interlevel transition instead of an intralevel transition in the commensurate fluctuation case. This pseudogap phenomenon has been clearly shown by neutron scattering.[18] In these optimally doped cases, the spin characteristic temperature T_c^* should become very close to the superconducting transition temperature T_c, to be consistent with neutron-scattering and NMR measurements. In the present theory, a superconducting transition will occur when spinons and holons are both condensed. Usually one finds $T_c^* > T_c$ at small doping. But when the spinons are condensed, the frustration effect on holons from the spin part (see next section) will be reduced too, which in turn is in favor of the Bose condensation of holons. In other words, T_c and T_c^* may correlate with each other. An optimal regime in the present theory may be properly defined as when T_c^* and T_c coincides. A further discussion of the superconducting transition will be presented elsewhere.

IV. TRANSPORT PROPERTIES

Due to spin-charge separation, the holon degree of freedom is to be solely responsible for the electron-transport phenomenon in this system. As noted before, the nonlocal phase A_{ij}^s in the holon Hamiltonian (1.3) will provide an unconventional scattering mechanism in two dimensions, as in contrast to the 1D case where it vanishes and holons simply behave like free particles. In the following, we will explore 2D transport properties under such an effective Hamiltonian H_h. Similar to the magnetic properties discussed in Sec. III, transport will be another crucial test for the experimental relevance of the present spin-charge separation theory.

For simplicity, we may consider H_h in the continuum limit at small doping. The validity of the continuum approximation will be discussed later. The corresponding continuum version of Eq. (1.3) has the form[96]

$$\tilde{H}_h = \int d^2\mathbf{r}\ \ h^+(\mathbf{r})\frac{(-i\nabla - \mathbf{A}^s)^2}{2m_t}h(\mathbf{r}), \tag{4.1}$$

where the holon mass $m_t = (\sqrt{2}t_h a^2)^{-1}$ and $\mathbf{A}^s$ is defined by $\mathbf{A}^s = \mathbf{A}_+^s + \mathbf{A}_-^s$, with

$$\mathbf{A}_\sigma^s = \frac{\sigma}{2}\int d^2\mathbf{r}'\frac{\hat{\mathbf{z}}\times(\mathbf{r}-\mathbf{r}')}{|\mathbf{r}-\mathbf{r}'|^2}\rho_\sigma^s(\mathbf{r}'). \tag{4.2}$$

Here $\rho_\sigma^s(\mathbf{r}) = b_\sigma^+(\mathbf{r})b_\sigma(\mathbf{r})$ is the local spinon density with spin index σ. Similarly to the lattice version [Eq. (1.5)], Eq. (4.2) describes fictitious π-flux quanta bound to spinons, and the sign $\sigma = \pm 1$ in front of the integration means that spinons with different spins carry flux tubes in opposite directions (see Fig. 5). In an unpolarized system, one has $\langle\rho_\uparrow^s\rangle = \langle\rho_\downarrow^s\rangle$ so that on average $\langle\mathbf{A}^s\rangle = 0$.

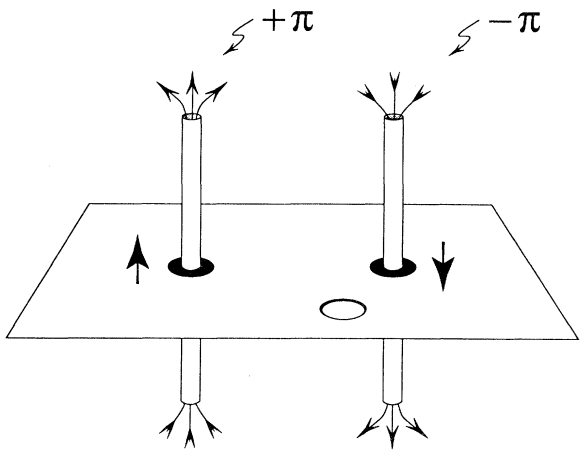

FIG. 5. Fictitious flux tubes attached to the spinons (solid circles) which are seen by the holon (open circle) on a 2D plane.

In other words, the scattering source as contributed by spinons may be regarded as a sort of fluctuating gauge field, and no T- and P-symmetry violations occur here.

Gauge-fluctuation-related scattering mechanisms have been intensively studied[35–37] within the framework of the uniform RVB state. So we need to distinguish the present gauge field $\mathbf{A}^s$ and those studied in the literature. Since the fictitious flux quanta are bound to spinons in the present case, let us first consider the local density distribution of spinons. At small doping, spinons are forming fluctuating AF domains, as discussed in Sec. III, within the spin correlation length $\xi > a$. For the purpose of illustration, an extreme case is shown in Fig. 6, where $\xi \sim a$

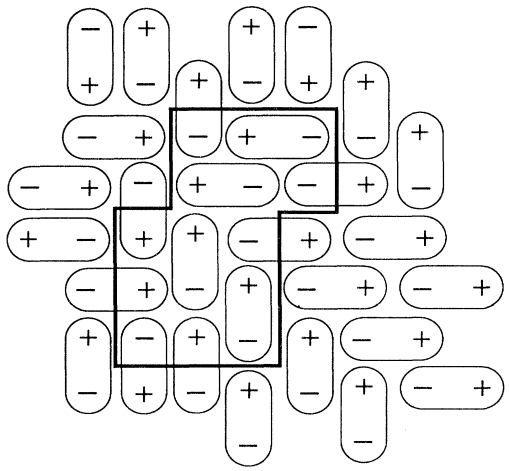

FIG. 6. An extreme case of short-range AF correlation. The + and − signs represent a spin configuration or, equivalently, an array of fictitious flux tubes bound to the spinons. The solid closed path cuts through those dimer pairs of spins and the total flux enclosed satisfies a perimeter law (see Ref. 98).

and only a pair of $\uparrow$ and $\downarrow$ spinons are bound together like a valence bond. $+$ and $-$ signs in Fig. 6 represent a spin configuration or, equivalently, directions of the π-flux quanta attached to spinons. If a holon moves about a closed path C as shown in Fig. 6, the accumulated flux will obviously have a large cancellation within the loop, with only the contribution from those near the path C whose pairs are cut by the loop. Then the mean-square accumulated flux will follow a perimeter law: $\propto L_C$ (L_C is the perimeter of the loop C). It is easy to observe that this perimeter law is generally true as long as there exists a short-range AF correlation, which is present at small doping and within a temperature range $k_BT < J$. This is in contrast to the gauge fluctuation in the uniform RVB state where fluctuating flux satisfies[36,97] an area law instead of a perimeter law. And the present flux problem is more similar to a random flux problem in the so-called "Meissner phase,"[98] where a perimeter law is present. But in the conventional case, the strength of the fluctuating flux is presumably weak so that the accumulated flux enclosed in a loop will become negligible when the loop is small enough. In this case only the long-distance behavior matters, and a perturbative approach may be applicable which is similar to a usual phonon-scattering problem.

However, in the present case, each flux tube attached to a spinon is quantized at π. It means that a slight deformation of the path C, with one spinon enclosed or excluded, could lead to an additional Berry phase $\pm\pi$ or a sign change of the wave function. A strong phase interference is therefore expected at a *short distance*[99] due to the high density of spinons at small doping. Such a short-distance effect can drastically change the nature of scattering mechanism which in the usual case would only involve long-wavelength processes. This is going to be a key distinction between the present theory and the usual gauge theories. We will see that such a short-range interference can lead to an exotic "localization" effect of holons, and result in a set of very interesting transport anomalous in longitudinal and transverse channels.

We begin by considering a single-holon problem. For a one-body problem, a Feynman path-integral formulation will become very useful. The transition amplitude for a holon to travel from a to b in space under the vector potential $\mathbf{A}^s$ is given by[100]

$$K(b,a) = \int_a^b \mathcal{D}\mathbf{r}(t)\, e^{i\mathcal{S}[b,a]}, \tag{4.3}$$

with the action

$$\mathcal{S}[b,a] = \int_{t_a}^{t_b} dt \left[\frac{m_t}{2}\dot{\mathbf{r}}^2 - \dot{\mathbf{r}}\cdot(\mathbf{A}^s_+ + \mathbf{A}^s_-)\right]. \tag{4.4}$$

By introducing the identities

$$\int \frac{d^2\boldsymbol{\lambda}}{(2\pi)^2} e^{i\boldsymbol{\lambda}\cdot(\mathbf{r}-\mathbf{r}_p)} = \delta(\mathbf{r}-\mathbf{r}_p), \tag{4.5a}$$

$$\int \frac{d^2\boldsymbol{\beta}}{(2\pi)^2} e^{i\boldsymbol{\beta}\cdot(\mathbf{r}-\mathbf{r}_q)} = \delta(\mathbf{r}-\mathbf{r}_q), \tag{4.5b}$$

$K(b,a)$ may be rewritten as

$$K(b,a) = \int_b^a \mathcal{D}\mathbf{r}(t)\mathcal{D}\mathbf{r}_p(t)\mathcal{D}\mathbf{r}_q(t) \int \mathcal{D}\boldsymbol{\lambda}\,(t) \int \mathcal{D}\boldsymbol{\beta}\,(t)\, e^{i\mathcal{S}_{\lambda\beta}[b,a]}, \tag{4.6}$$

in which

$$\mathcal{S}_{\lambda\beta}[b,a] = \int_{t_a}^{t_b} dt \left[\frac{m_h}{2}\dot{\mathbf{r}}^2 + \frac{m_p}{2}\dot{\mathbf{r}}_p^2 + \frac{m_q}{2}\dot{\mathbf{r}}_q^2\right] - \int_a^b d\mathbf{r}_p\cdot\mathbf{A}^s_+(\mathbf{r}_p) - \int_a^b d\mathbf{r}_q\cdot\mathbf{A}^s_-(\mathbf{r}_q) + \int_{t_a}^{t_b} dt[\boldsymbol{\lambda}(t)\cdot(\mathbf{r}-\mathbf{r}_p) + \boldsymbol{\beta}(t)\cdot(\mathbf{r}-\mathbf{r}_q)], \tag{4.7}$$

where $m_h + m_p + m_q = m_t$. Extra degrees of freedom are thus introduced in Eq. (4.6). Without the last term involving the Lagrangian multipliers $\boldsymbol{\lambda}$ and $\boldsymbol{\beta}$, $\mathcal{S}_{\lambda\beta}[b,a]$ in Eq. (4.7) would simply describe three independent particles: a free holon with mass m_h known as h species, and p and q species which interact with the vector potentials $\mathbf{A}^s_+$ and $\mathbf{A}^s_-$, respectively. The fields $\boldsymbol{\lambda}$ and $\boldsymbol{\beta}$ play the role to recombine these three species together as a real holon, and thus effectively eliminate the additional degrees of freedom in the end.

So far no approximation has been made. By introducing p and q degrees of freedom, the effects of $\mathbf{A}^s_+$ and $\mathbf{A}^s_-$ are separated. In terms of Eq. (4.2), $\mathbf{A}^s_\sigma$ may be rewritten as $\mathbf{A}^s_\sigma = \sigma\bar{\mathbf{A}}^s + \delta\mathbf{A}^s_\sigma$, where

$$\bar{\mathbf{A}}^s = \frac{B_s}{2}(\hat{\mathbf{z}}\times\mathbf{r}), \tag{4.8}$$

with $B_s = (1-\delta)\pi/2$, and $\delta\mathbf{A}^s_\sigma$ has the same form as Eq. (4.2) but with ρ^s_σ replaced by $\delta\rho^s_\sigma = \rho^s_\sigma - \langle\rho^s_\sigma\rangle$. A similar procedure has been used in dealing with the topological phase $\mathbf{A}^h$ in spinon system (cf. Sec. III), and is familiar in an anyon problem.[82,83] Here $\sigma\bar{\mathbf{A}}^s$ describes a mean-field effect with the flux quanta smeared out uniformly in space. And $\delta\mathbf{A}^s_\sigma$ represents the fluctuation of the flux quanta due to the density fluctuation of spinons with spin index σ. In the following, we shall show that,

to a leading order of approximation, the effect of $\delta \mathbf{A}_\sigma^s$ in the action (4.7) could be effectively represented by a relaxation of the binding constraint enforced by $\boldsymbol{\lambda}$ and $\boldsymbol{\beta}$ within a scale of the cyclotron length d_c of p and q species (under the fictitious field B_s). Under such an approximation a renormalized holon will be a composite particle of a bare holon and the p and q species which are in the cyclotron orbitals. Below we elaborate this approximation.

Due to the symmetry, one only needs to focus on the p species. Let us consider an arbitrary closed path C on a 2D plane (Fig. 7). The contribution of $\mathbf{A}_+^s$ to the transition amplitude in Eq. (4.6) for such a path will be a gauge-invariant phase:

$$\oint_C d\mathbf{r}_p \cdot \mathbf{A}_+^s = \oint_C d\mathbf{r}_p \cdot \bar{\mathbf{A}}^s + \oint_C d\mathbf{r}_p \cdot \delta \mathbf{A}_+^s. \tag{4.9}$$

Equation (4.9) may be further rewritten as

$$\oint_C d\mathbf{r}_p \cdot \mathbf{A}_+^s = \oint_{C_p} d\mathbf{r}_p \cdot \bar{\mathbf{A}}^s, \tag{4.10}$$

in which a path C_p is introduced such that

$$\left(\oint_{C_p} - \oint_C \right) (d\mathbf{r}_p \cdot \bar{\mathbf{A}}^s) = \oint_C d\mathbf{r}_p \cdot \delta \mathbf{A}_+^s$$

$$= \pi \Delta N_c^{\uparrow}. \tag{4.11}$$

Here the path C_p as shown in Fig. 7 is a deformation of the path C to account for the fluctuation of $\delta \mathbf{A}_s^+$ in terms of the mean-field $\bar{\mathbf{A}}^s$. In second line of Eq. (4.11), $\Delta N_c^{\uparrow}$ represents the total fluctuating $\uparrow$ spinon number (with regard to the average one) enclosed by the path C, and such a term describes the total *fluctuating* fluxes bound to $\uparrow$ spinons as deduced from the right-hand-side integral in the first line. So the flux enclosed between the paths C and C_p under a uniform field B_s will represent the fluctuation of the flux quanta attached to $\uparrow$ spinons inside the path C. In the following we shall point out that $\pi \Delta N_c^{\uparrow}$ should satisfy the perimeter law discussed at the beginning of this section.

In the spin background, there is no density fluctuation due to the no-double-occupancy constraint, and locally an increase of $\uparrow$ spinons is always compensated by a decrease of $\downarrow$ spinons. Thus the distribution of $\uparrow$ spinons will actually reflect that of all spins in the hole-absent region. With the presence of a short-range AF correlation (the correlation length $\xi > a$), excess and deficit of $\uparrow$ spinons are neighboring to each other (the $\xi \sim a$ case is shown in Fig. 6). In such a "Meissner phase," the net contribution to $\Delta N_c^{\uparrow}$ mainly comes from $\uparrow$ spinons close to the path C, and $\Delta N_c^{\uparrow}$ should satisfy a perimeter law instead of an area law as explained before. Correspondingly, the path C_p should be always near the path C to account for $\Delta N_c^{\uparrow}$ in terms of Eq. (4.11), as shown in Fig. 7. An average separation d_p of C_p from C may be estimated as follows: $\pi d_p^2 \times B_s \sim$ one flux quanta $= \pi$,

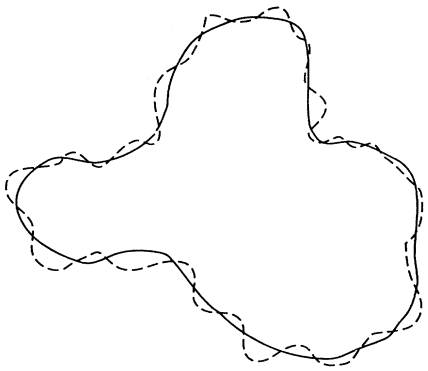

FIG. 7. An arbitrary closed path C of a holon (solid one) and a corresponding path C_p for p species (dashed one).

which leads to $d_p \sim 1/\sqrt{B_s} = d_c$ — the cyclotron length under B_s.

So after one replaces $\mathbf{A}_+^s$ by $\bar{\mathbf{A}}^s$ in Eq. (4.7), the fluctuation effect can be taken into account by deforming the path of p species from C to C_p. The deviation of C_p from C depends on the detailed fluctuation of $\mathbf{A}_+^s$. But if the temperature is sufficiently higher than the spinon characteristic energy scale (the broadening of the Landau level in the spinon spectrum), the path C_p shown in Fig. 7 may be reasonably regarded as a random one, with an average separation d_c from the path C. This effectively means that the binding constraints of h, p, and q implemented by the Lagrangian fields $\boldsymbol{\lambda}$ and $\boldsymbol{\beta}$ have been relaxed within a scale $\sim d_c$. Here the kinetic energy cost of the deformation path C_p is neglected due to the smallness of d_c. In the weak gauge-fluctuation case, d_c could be too large for the present approximation to be valid.

Thus, the motion of a holon under the influence of the gauge field $\mathbf{A}^s$ can be effectively described as a bare holon bound to a pair of auxiliary species, p and q, which are undergoing cyclotron motions in opposite directions. These p and q species reflect a "localized" effect caused by the phase interference at short distances. As p and q are confined in the Landau levels, a large degeneracy is involved here. In real space, such a renormalized holon would look like a polaron, and behave like a diffusive particle in the absence of external fields. This peculiar structure will decide a unique transport phenomenon.

The generalization of the above scheme to a many-body case is straightforward. Here one has to be cautious about the statistics of each species in the many-body case. A holon as a composite particle of h, p, and q species has to satisfy the (hard-core) bosonic statistics. Thus a symmetric choice would be that the h species corresponds to a boson while the p and q species are spinless fermions (so that the hard-core condition can be automatically realized). Then the effective many-body Lagrangian as a generalization of the one-body approximation discussed above can be written in the functional-integral formalism as

$$\mathcal{L}_h = \int d^2\mathbf{r}\left\{h^\dagger\partial_\tau h + p^\dagger\partial_\tau p + q^\dagger\partial_\tau q + \lambda(p^\dagger p - h^\dagger h) + \beta(q^\dagger q - h^\dagger h)\right\}$$
$$+ \int d^2\mathbf{r}\left\{h^\dagger(\mathbf{r})\frac{(-i\nabla + \boldsymbol{a}^{\rm ext})^2}{2m_h}h(\mathbf{r}) + p^\dagger(\mathbf{r})\frac{(-i\nabla - \bar{\mathbf{A}}^s)^2}{2m_p}p(\mathbf{r}) + q^\dagger(\mathbf{r})\frac{(-i\nabla + \bar{\mathbf{A}}^s)^2}{2m_q}q(\mathbf{r})\right\}, \quad (4.12)$$

in which $\boldsymbol{a}^{\rm ext}$ is an external vector potential. And the fields $h(\mathbf{r})$, $p(\mathbf{r})$, and $q(\mathbf{r})$ are in the coherent representation. The Lagrangian multipliers $\lambda(\mathbf{r})$ and $\beta(\mathbf{r})$ enforce the binding constraint

$$h^\dagger(\mathbf{r})h(\mathbf{r}) = p^\dagger(\mathbf{r})p(\mathbf{r}) = q^\dagger(\mathbf{r})q(\mathbf{r}), \quad (4.13)$$

in a length scale larger than d_c. An ultraviolet momentum cutoff $\Lambda = 1/d_c$ is then implied in λ and β fields in the Lagrangian $\mathcal{L}_h$. The masses m_h, m_p, and m_q are determined up to where their total summation is equal to m_t. The value of each individual mass has to be decided beyond the present approximation, and this uncertainty will not affect the general conclusions we shall draw from the Lagrangian $\mathcal{L}_h$.

Therefore, we obtain an effective long-wavelength Lagrangian (4.12) for holons after the short-distance phase interference is carefully considered. This is a rather unusual Lagrangian because there are three auxiliary species involved. But it is not derived for the first time here. A similar one has already been found[74] in the scheme-1 flux-binding state (see Sec. II) through a different method. Even though the approximations involved in these two states are different, their origins are quite similar and it is not surprising to find their normal states to be so close. In fact, the structures of two effective Lagrangians for holons are identical, except that B_s is twice larger in Ref. 74 and the h field is a fermionic one there. A larger B_s in Ref. 74 is due to the fact that the π-flux phase ϕ^0_{ij} has been incorporated into B_s at the continuum limit. These differences do not change the canonical behaviors described below.

The effective Lagrangian $\mathcal{L}_h$ determines an anomalous transport phenomenon[74] which amazingly matches the essential characteristics of the optimally doped cuprates. We shall outline the main results in the following. For detailed discussions, one is referred to Ref. 74. $\mathcal{L}_h$ can be treated by the standard gauge-theory approach. Here it is even simpler for lacking the transverse fields. It is easy to show that the longitudinal fields λ and β will enforce the following current constraint among h, p, and q species:

$$\mathbf{J}^l_h = \mathbf{J}^l_p = \mathbf{J}^l_q, \quad (4.14)$$

where the superscript l implies the longitudinal channel. This constraint is consistent with the density constraint [Eq. (4.13)]. It is important to note that there is no similar current constraint in the transverse channel due to the absence of transverse gauge fields. The total response to an external electromagnetic field will be related to each species through Eq. (4.14). And different combination rules will thus be found in the longitudinal and transverse transport channels, which will lead to a distinctive Hall-angle behavior.

The scattering rates of h, p, and q are decided by their coupling with the longitudinal gauge fields λ and β in Eq. (4.12), whose dynamics are in turn determined by coupling to h, p, and q species. A self-consistent treatment is required here. Due to the peculiar feature that p and q stay in the Landau level, one finds that the scattering rate for p and q goes linearly in temperature, i.e., $\frac{\hbar}{\tau_s} = 2\kappa k_B T$, where $\kappa \sim O(1)$ is independent of the coupling constant (the masses) and only has a weak doping dependence (and $\frac{1}{\tau_s} \propto \omega$ is also found when $\hbar\omega > k_B T$). And for the h species, the scattering rate has a T^2 behavior: $\frac{\hbar}{\tau_h} \propto \frac{(k_B T)^2}{t_h}$. In terms of the constraint Eq. (4.14), the total longitudinal resistivity can be determined[74] and at $k_B T \ll t_h$ it is dominant by $1/\tau_s$ so that $\rho \propto T$. The linear-T resistivity in the cuprates is indeed found[2] to be related to a linear-T relaxation rate. Particularly, the coefficient is roughly around a numerical factor of 2 for all the optimal materials.[2] This is a very interesting feature and is *quantitatively* consistent with the present theory, where the coupling-independent coefficient $2\kappa \sim 2$ is determined by the unique structure in the scheme. The transverse resistivity ρ_{xy} can be also obtained, and as noted before the distinctive combination rules in the longitudinal and transverse channels will lead to new consequences. Namely, the Hall angle Θ as defined by $\cot\Theta = \rho/\rho_{yx}$ is found to be related to the second scattering rate $1/\tau_h$: $\cot\Theta \propto 1/\tau_h \propto T^2$. Consequently the Hall coefficient R_H follows a $1/T$ behavior. The involvement of a second scattering rate $\propto T^2$ in the Hall angle for high-T_c cuprates was pointed out by the Princeton group[4,5] based on the analysis of the experimental data. The effective Lagrangian in Eq. (4.12) provides a microscopic theory for it. A magnetoresistance with $\Delta\rho/\rho \sim T^{-4}$ dependence has been also predicted[74] in the longitudinal channel, which has been recently observed[6] in YBCO (we note that the overall sign is uncertain in the theory while experimentally it is found to be positive). Due to the "localized" effect of holons, a strongly doping-dependent thermopower has been obtained in the present framework, which also agrees well with the experimental measurements in the high-T_c cuprates.

The transport properties determined by the effective Lagrangian $\mathcal{L}_h$ may be called the canonical ones, which well account for the optimally doped cuprates. In the following we briefly discuss the condition for a deviation from such a canonical case in the present theory. The key assumption involved in deriving Eq. (4.12) from $\tilde{H}_h$ is the randomness of the flux quanta movement near the path C shown in Fig. 7, which leads to uncorrelated segments along the path C_p so that p and q can be effectively

treated as detached from h at a scale of d_c. In this case, the detailed spin dynamics becomes irrelevant. In the optimal doped cuprates, the spinon LLL broadening is very sharp (cf. Sec. III) so that the above condition may be always satisfied at the normal-state temperature. For underdoped YBCO, however, the LLL broadening is quite large, and when the thermal energy is less than it the detailed spin dynamics could get involved in C_p, especially when $T \sim T_c^*$, and spinons begin to condensate into the energy bottom. In this case, C_p may not be treated as a random one with regard to C, and the present approximation could break down. As a consequence, a deviation from the canonical transport behaviors is expected below some temperature scale, which should be correlated with T_c^*. Experimentally, such a correlation between the transport and the "spin gap" is indeed found[101,102] in the underdoped YBCO system. Furthermore, at sufficiently small doping, the transport properties described by Eq. (4.12) itself can also deviate from the canonical behavior as discussed in Ref. 74.

Finally, we would like to make a comment on the continuum approximation of H_h. At small doping, the continuum approximation can be well justified for the spinon Hamiltonian H_s because A_{ij}^h in it is vanishingly small. In the present holon case, however, the strong fluctuation effect at short distances is very important, even though $\langle A_{ij}^h \rangle = 0$. Thus one would expect the lattice effect to be involved even at small doping. So far we have not been able to include such a lattice effect. Nevertheless, as the phase interference at short distances is not a coherent effect, the role of the lattice effect may not be really crucial. Furthermore, p and q are just auxiliary particles to take care of the phases interference, which can be introduced in the continuum space even when lattice is included. A further study is still needed.

V. CONCLUSION

In this paper, we have obtained the spin-charge separation scheme based on a saddle-point state of the t-J model. In this saddle-point state, we find a deconfinement of spin and charge degrees of freedom at finite doping in the 2D case, where the transverse gauge field as the confinement force is gapped. Such a gap disappears at half-filling, where spinons are presumably confined to form spin-1 excitations, and a long-range AF order has been recovered. This saddle-point state has been also shown to reproduce the known asymptotic spin-spin correlation in one dimension at both half-filling and finite doping. Thus, in some important limits where the behaviors of the t-J model are known, the present state has produced the right results. These constitute an important check for the strongly correlated model where the conventional approximation breaks down.

The most interesting properties have been found at finite doping in the 2D case, when spin and charge become deconfined. In this regime, the saddle-point state becomes meaningful due to the suppression of the gauge fluctuation, and spinons and holons can be appropriately treated as separated systems in terms of conventional approaches. We have shown that in this saddle-point state there still exist some exotic residual couplings between spin and charge degrees of freedom, in spite of the spin-charge deconfinement. These couplings are nonlocal in the sense that spinons can feel the existence of holons nonlocally by seeing some fictitious flux quanta bound to the latter and vice versa. Different from a usual electron-phonon system where the coupling is a single *interactive* term, spinons and holons here are scattered by each other in distinctive forms. These scattering forces lead to anomalous spin dynamics and transport properties in the present system. For example, a sharp AF peak centered at $\mathbf{Q}_0$ is exhibited in the imaginary dynamic spin susceptibility with an energy scale much smaller than the exchange energy J. The width of such an AF peak in $\mathbf{q}$ space is determined by the doping concentration in a form $\propto \sqrt{\delta}$, which is temperature independent but increases with energy transfer. The NMR spin relaxation rate of nuclear spin due to coupling with such a magnetic fluctuation shows a non-Korringa behavior for planar Cu nuclei and a strong suppression for planar O nuclei. Furthermore, we have found a characteristic temperature T_c^* below which all these AF anomalies get suppressed, in resemblance to a "spin-gap" system if the superconducting temperature $T_c < T_c^*$ and $T_c < T < T_c^*$. Incommensurate AF fluctuations have also been found in this system at a *higher*-energy scale. For the charge degree of freedom, we have demonstrated that the scattering from the spinon background leads to a strong phase interference at short distances for holons, and an effective long-wavelength Lagrangian is derived. Such a Lagrangian has been found to give the following canonical transport phenomena: resistivity $\rho \sim T$ with $\hbar/\tau \simeq 2k_B T$, Hall angle $\cot\theta_H \propto 1/\tau_h \propto T^2$, magnetoresistance $\Delta\rho/\rho \propto T^{-4}$, and a strong doping dependence of the thermopower.

The magnetic and transport properties of the present spin-charge separation state share amazing similarities with those found in the high-T_c cuprates, as discussed in the context of the paper. Based on the theory, a consistent picture can be conjecturally formed for the normal state of the cuprates. The optimally doped materials can be defined as $T_c \sim T_c^*$, where the *commensurate* AF fluctuation energy scale becomes very small, maybe indetectable in terms of the present neutron-scattering resolution. Such a small energy scale is a unique feature of the present state, and as discussed in this context, NMR and neutron-scattering data in both metallic LSCO and $YB_2Cu_3O_7$ can be reconciled here. And in the transport channel, the canonical behaviors are exhibited in agreement with the transport measurements. A larger commensurate AF fluctuation energy scale can be realized at a smaller doping regime, where holons tend to be localized, and the interlayer coupling in YBCO could further help the broadening of the energy scale. In this regime, a commensurate AF fluctuation may become observable in neutron scattering as in underdoped YBCO, and pseudo-spin-gap behaviors will also show up in both the neutron-scattering and NMR spin relaxation rate below T_c^* ($> T_c$). In this case, a deviation from the canonical behaviors is expected in the transport channel below a temperature scale around T_c^*. We note that in the

present theory, there is no direct experimental input except that the underlying t-J model is widely perceived as a simplified description of the copper-oxide layer in the cuprates. This becomes a compelling fact as so many important experimental features are naturally exhibited in the present state. We have pointed out in the Introduction that spin-charge separation is the key for all these delicate magnetic and transport anomalies to appear.

Two other important issues remain to be clarified in the present spin-charge separation scheme. One is about the single-electron properties, particularly the location of the Fermi surface, and the other is about the superconducting condensation in this framework. Since an electron is described as composed of two *bosonic* holons and spinons, the accompanied nonlocal phase fields in Eq. (1.6) will play a central role in restoring the fermionic properties of the electron. As outlined in the Introduction, nonlocal phase fields will be responsible for an electronic Fermi surface satisfying the Luttinger volume theorem as well as a finite pairing order parameter $\langle c^\dagger_{i\uparrow} c^\dagger_{j\downarrow} \rangle$ (and its symmetry) when both holons and spinons are Bose condensed. We shall discuss these important problems in follow-up papers.

ACKNOWLEDGMENTS

The authors acknowledge helpful discussions with T.K. Lee, D. Frenkel, and A. Chubukov. Z.Y.W. would like to thank G. Aeppli, G. Baskaran, B. Doucot, M. Imada, S. Liang, Y. Ren, A. Sokol, O. Starykh, Z.B. Su, C. Varma, R.E. Walstedt, and L. Yu for stimulating conversations. The present work is supported partially by Texas Advanced Research Program under Grant No. 3652182, a grant from the Robert Welch foundation, and by the Texas Centre for Superconductivity at the University of Houston.

[1] For a review, see Y. Iye, in *Physical Properties of High Temperature Superconductors*, edited by P.M. Ginsberg (World Scientific, Singapore, 1992), Vol. 3, p. 159.
[2] For a review, see D.B. Tanner and T. Timusk, in *Physical Properties of High Temperature Superconductors* (Ref. 1), Vol. 3, p. 363.
[3] For a review, see N.P. Ong, in *Physical Properties of High Temperature Superconductors* (Ref. 1), Vol. 2, p. 459.
[4] P.W. Anderson, Phys. Rev. Lett. **67**, 2092 (1991).
[5] T.R. Chien, Z.Z. Wang, and N.P. Ong, Phys. Rev. Lett. **67**, 2088 (1991).
[6] J.M. Harris, Y.F. Yan, N.P. Ong, and P.W. Anderson (unpublished).
[7] For a review, see A.B. Kaiser and C. Uher, in *Studies of High Temperature Superconductors*, edited by A. Narlikar (Nora Science Publishers, New York, 1991).
[8] For a review, see C.H. Pennington and C.P. Slichter, in *Physical Properties of High Temperature Superconductors* (Ref. 1), Vol. 2, p. 269.
[9] For a review, see R.J. Birgeneau and G. Shirane, in *Physical Properties of High Temperature Superconductors* (Ref. 1), Vol. 1, p. 151.
[10] R.E. Walstedt *et al.*, Phys. Rev. B **38**, 9299 (1988).
[11] F. Mila and T.M. Rice, Physica C **17**, 561 (1989).
[12] B.S. Shastry, Phys. Rev. Lett. **63**, 1288 (1989).
[13] P.C. Hammel *et al.*, Phys. Rev. Lett. **63**, 1992 (1989).
[14] A.J. Millis, H. Monien, and D. Pines, Phys. Rev. B **42**, 167 (1990).
[15] N. Bulut, D. Hone, and D.J. Scalapino, and N.E. Bickers, Phys. Rev. Lett. **64**, 2723 (1990).
[16] R.J. Birgeneau *et al.*, Phys. Rev. B **38**, 6614 (1988); T.R. Thurston *et al.*, *ibid.* **40**, 4585 (1989); G. Shirane *et al.*, Phys. Rev. Lett. **63**, 330 (1989).
[17] S.M. Hayden *et al.*, Phys. Rev. Lett. **66**, 821 (1991).
[18] S-W. Cheong *et al.*, Phys. Rev. Lett. **67**, 1791 (1991); T.E. Maston *et al.*, *ibid.* **68**, 1414 (1992); **71**, 919 (1993); T.R. Thurston *et al.*, Phys. Rev. B **46**, 9128 (1992); M. Matsuda *et al.*, *ibid.* **49**, 6958 (1994).
[19] J. Rossat-Mignod *et al.*, Physica B **163**, 4 (1990); **180&187**, 383 (1992).
[20] J.M. Tranquanda *et al.*, Phys. Rev. B **46**, 5561 (1992); B.J. Sternlieb *et al.*, *ibid.* **47**, 5320 (1993).
[21] H.A. Mook *et al.*, Phys. Rev. Lett. **70**, 3490 (1993).
[22] R.E. Walstedt, B.S. Shastry, and S-W. Cheong, Phys. Rev. Lett. **72**, 3610 (1994).
[23] V. Barzykin, D. Pines, and D. Thenlen, Phys. Rev. B **50**, 16 052 (1994).
[24] C.G. Olson, R. Liu, A. Yang, D.W. Lynch, A.J. Arko, R.S. List, B. Veal, Y. Chang, P. Jiang, and A. Paulikas, Science **245**, 731 (1989); Phys. Rev. B **42**, 381 (1990).
[25] D.S. Dessau, Z.-X. Shen, D.M. King, D.S. Marshall, L.W. Lombardo, P.H. Pichinson, A.G. Loeser, J. DiCarlo, C.-H. Park, A. Kapituluik, and W.E. Spicer, Phys. Rev. Lett. **71**, 2781 (1993), and the references therein.
[26] C.M. Varma, P.B. Littlewood, S. Schmitt-Rink, E. Abrahams, and A.E. Ruckenstein, Phys. Rev. Lett. **63**, 1996 (1989); **64**, 497(E) (1990).
[27] P.B. Littlewood, J. Zaanen, G. Aeppli, and H. Monien, Phys. Rev. B **48**, 487 (1993).
[28] D.M. Newns, C.C. Tsuei, R.P Huebener, P.J.M. van Bentum, P.C. Pattnaik, and C.C. Chi, Phys. Rev. Lett. **73**, 1695 (1994).
[29] Q. Si, Y. Zha, K. Levin, and J.P. Lu, Phys. Rev. B **47**, 9055 (1993).
[30] T. Imai *et al.*, Phys. Rev. Lett. **70**, 1002 (1993).
[31] A. Sokol, E. Gagliano, and S. Bacci, Phys. Rev. B **47**, 14 646 (1993).
[32] P.W. Anderson, Science, **235**, 1196 (1987); in *Frontiers and Borderlines in Many Particle Physics*, edited by P.A. Broglia and J.R. Schrieffer (North-Holland, Amsterdam, 1987); P.W. Anderson and Y. Ren, in *High Temperature Superconductivity*, edited by K.S. Bedell *et al.* (Addison-Wesley, Redwood City, 1990); P.W. Anderson, Phys. Rev. Lett. **64**, 1839 (1990); **65**, 2306 (1990).
[33] S.A. Kivelson, D.S. Rokhsar, and J.R. Sethna, Phys. Rev. B **35**, 8865 (1987).
[34] G. Baskaran and P.W. Anderson, Phys. Rev. B **37**, 580 (1988).

[35] L.B. Ioffe and A.I. Larkin, Phys. Rev. B **39**, 8988 (1989).
[36] N. Nagaosa and P.A. Lee, Phys. Rev. Lett. **64**, 2450 (1990); P.A. Lee and N. Nagaosa, Phys. Rev. B **46**, 5621 (1992).
[37] L.B. Ioffe and P.B. Wiegmann, Phys. Rev. Lett. **65**, 653 (1990); L.B. Ioffe and G. Kotliar, Phys. Rev. B **42**, 10 348 (1990).
[38] E. Fradkin, *Field Theory of Condensed Matter Systems* (Addison-Wesley, Redwood City, 1991).
[39] See A.M. Polyakov, *Gauge Fields and Strings* (Harwood Academic Publishers, New York, 1987).
[40] M. Ogata and H. Shiba, Phys. Rev. B **41**, 2326 (1990); H. Shiba and M. Ogata, Prog. Theor. Phys. Suppl. **108**, 265 (1992).
[41] P.W. Anderson, Int. J. Mod. Phys. B **4**, 181 (1990).
[42] Z.Y. Weng, D.N. Sheng, C.S. Ting, and Z.B. Su, Phys. Rev. Lett. **67**, 3318 (1991); Phys. Rev. B **45**, 7850 (1992).
[43] Z.Y. Weng, C.S. Ting, and T.K. Lee, Phys. Rev. B **43**, 3790 (1991).
[44] F.D.M. Haldane, J. Phys. C **14**, 2585 (1981).
[45] H. Frahm and V.C. Korepin, Phys. Rev. B **42**, 10 553 (1990).
[46] H.J. Schulz, Phys. Rev. Lett. **64**, 2831 (1990).
[47] Y. Ren and P.W. Anderson, Phys. Rev. B **48**, 16 662 (1993).
[48] F.C. Zhang and T.M. Rice, Phys. Rev. B **37**, 3759 (1988).
[49] C. Gros, R. Joynt, and T.M. Rice, Phys. Rev. B **36**, 8910 (1987).
[50] S. Chakravarty, B.I. Halperin, and D.R. Nelson, Phys. Rev. Lett. **60**, 1057 (1988); A.V. Chubukov, S. Sachdev, and J. Ye, Phys. Rev. B **49**, 11 919 (1994).
[51] D.P. Arovas and A. Auerbach, Phys. Rev. B **38**, 316 (1988).
[52] E.H. Lieb and F.Y. Wu, Phys. Rev. Lett. **20**, 1445 (1968).
[53] I.A. Affleck and J.B. Marston, Phys. Rev. B **37**, 3774 (1988).
[54] P. Jordan and E. Wigner, Z. Phys. **47**, 631 (1928).
[55] G. Baskaran, in *Two-dimensional Strong Correlation System*, Beijing Workshop, 1988, edited by Z.B. Su *et al.* (Gordon and Breach, New York, 1988); E. Fradkin, Phys. Rev. Lett. **63**, 322 (1989); Y.R. Wang, Phys. Rev. B **43**, 3786 (1991).
[56] Z.Y. Weng, Phys. Rev. B **50**, 13 837 (1994).
[57] W. Marshall, Proc. R. Soc. London A **232**, 48 (1955).
[58] Z.Y. Weng, D.N. Sheng, and C.S. Ting, Mod. Phys. Lett. B **8**, 1353 (1994).
[59] S.E. Barnes, J. Phys. F **6**, 1375 (1976); P. Coleman, Phys. Rev. B **29**, 3035 (1984); N. Read and D. Newns, J. Phys. C **16**, 3237 (1983).
[60] Z. Zou and P.W. Anderson, Phys. Rev. B **37**, 627 (1988).
[61] For a review, see P.A. Lee, in *High Temperature Superconductivity*, edited by K.S. Bedell *et al.* (Addison-Wesley, Redwood City, 1990).
[62] M. Grilli and G. Kotliar, Phys. Rev. Lett. **64**, 1170 (1990).
[63] S. Liang and N. Trivedi, Phys. Rev. Lett. **64**, 232 (1990).
[64] N. Trivedi and D.M. Ceperley, Phys. Rev. B **40**, 2737 (1989).
[65] Y.R. Wang, Phys. Rev. B **46**, 151 (1992).
[66] G.S. Canright, S.M. Girvin, and A. Brass, Phys. Rev. Lett. **63**, 2291 (1989); **63**, 2295 (1989); C. Kallin, Phys. Rev. B **48**, 13 742 (1993).
[67] R.B. Laughlin, Science, **242**, 525 (1988); Phys. Rev. Lett. **60**, 2677 (1988).
[68] Z.Y. Weng, D.N. Sheng, and C.S. Ting, Phys. Rev. B **49**, 607 (1994).
[69] P. Lederer, D. Poilblanc, and T.M. Rice, Phys. Rev. Lett. **63**, 1519 (1989); Y. Hasegawa, P. Lederer, T.M. Rice, and P.B. Wiegmann, *ibid.* **63**, 907 (1989).
[70] P.B. Wiegmann, Phys. Rev. Lett. **65**, 2070 (1990); J. P. Rodriguez and B. Doucot, Phys. Rev. B **42**, 8724 (1990); **45**, 971 (1992).
[71] Y. Hasegawa, O. Narikiyo, K. Kuboki, and H. Fukuyama, J. Phys. Soc. Jpn. **59**, 822 (1990).
[72] D. Schmeltzer, Phys. Rev. B **48**, 10 466 (1993).
[73] Z. Zou, J.L. Levy, and R.B. Laughlin, Phys. Rev. B **45**, 993 (1992); A.M. Tikofsky, R.B. Laughlin, and Z. Zou, Phys. Rev. Lett. **69**, 3670 (1992).
[74] Z.Y. Weng, D.N. Sheng, and C.S. Ting, Phys. Rev. B **50**, 9470 (1994).
[75] F.D.M. Haldane and H. Levine, Phys. Rev. B **40**, 7340 (1989).
[76] C. Gros, S.M. Girvin, G.S. Canright, and M.D. Johonson, Phys. Rev. B **43**, 5883 (1991).
[77] A. Luther and I. Peschel, Phys. Rev. B **12**, 3908 (1975).
[78] See I. Affleck, in *Fields, Strings and Critical Phenomena*, edited by E. Bezin and J. Zinn-Justin (North-Holland, Amsterdam, 1990).
[79] B.S. Shastry, Mod. Phys. Lett. B **6**, 1427 (1992).
[80] Y.C. Chen and T.K. Lee (unpublished).
[81] B. Shraiman and E. Siggia, Phys. Rev. Lett. **60**, 740 (1988).
[82] C.B. Hanna, R.B. Laughlin, and A.L. Fetter, Phys. Rev. B **40**, 8745 (1989); A.L. Fetter, C.B. Hanna, and R.B. Laughlin, *ibid.* **39**, 9679 (1989); Q. Dai, J.L. Levy, A.L. Fetter, C.B. Hanna, and R.B. Laughlin, *ibid.* **46**, 5642 (1992).
[83] Y.H. Chen, F. Wilczek, E. Witten, and B.I. Halperin, Int. J. Mod. Phys. B **3**, 1001 (1989).
[84] J.L. Levy and R.B. Laughlin, Phys. Rev. B **50**, 7107 (1994).
[85] T. Moria, Prog. Theor. Phys. **28**, 371 (1962).
[86] P. Bourges, P.M. Gehring, B. Hennion, and A.H. Moudden, Phys. Rev. B **43**, 8690 (1991).
[87] H. Chou, J.M. Tranquada, G. Shirane, T.E. Mason, W.J.L. Buyers, S. Shamoto, and M. Sato, Phys. Rev. B **43**, 5554 (1991).
[88] M. Takigawa, A.P. Reyes, P.C. Hammel, J.D. Thmpson, R.H. Heffner, Z. Fisk, and K.C. Ott, Phys. Rev. B **43**, 247 (1991).
[89] A. Millis and H. Monien, Phys. Rev. Lett. **70**, 2810 (1993); **71**, 210(E) (1993).
[90] B.L. Altshuler and I.B. Ioffe, Solid State Commun. **82**, 253 (1993).
[91] M.U. Ubbens and P.A. Lee, Phys. Rev. B **50**, 438 (1994).
[92] P. Monthoux, A. Balatsky, and D. Pines, Phys. Rev. Lett. **67**, 3448 (1991); Phys. Rev. B **46**, 14 803 (1992).
[93] B. Shraiman and E. Siggia, Phys. Rev. Lett. **62**, 1564 (1988).
[94] C.L. Kane, P.A. Lee, T.K. Ng, B. Chakraborty, and N. Read, Phys. Rev. B **41**, 2653 (1990).
[95] Z.Y. Weng, Phys. Rev. Lett. **66**, 2156 (1991).
[96] As usual, $\exp(iA^s_{ij})$ in Eq. (1.3) will be expanded up to the quadratic term of A^s_{ij}. The leading term in $\tilde{H}_h$ will be a tight-binding model with the presence of π-flux per plaquette. A continuum expansion near the band bottom will yield an additional $\sqrt{2}$ mass enhancement due to the flux ϕ^0_{ij} in H_h.
[97] M.U. Ubbens and P.A. Lee, Phys. Rev. B **49**, 13 049

(1994).
[98] G. Gavazzi, J.M. Wheatley, and A.J. Schofield, Phys. Rev. B **47**, 15 170 (1993).
[99] It is interesting to note that a characteristic short-distance scale under a uniform magnetic field is the cyclotron length which can be defined as the radius of a circle which encloses a flux just equal to π: $\pi \times$ (cyclotron length)$^2 \times$ magnetic field $= \pi$. Beyond the cyclotron length, phase destruction could greatly suppress the amplitude of the wave packet.
[100] See R.P. Feynman and A.R. Hibbs, *Path Integrals and Quantum Mechanics* (McGraw-Hill, New York, 1965).
[101] T. Ito, K. Takenaka, and S. Uchida, Phys. Rev. Lett. **70**, 3995 (1993).
[102] S.L. Cooper and K.E. Gray, in *Physical Properties of High Temperature Superconductors* (Ref. 1), Vol. 4, p. 61.